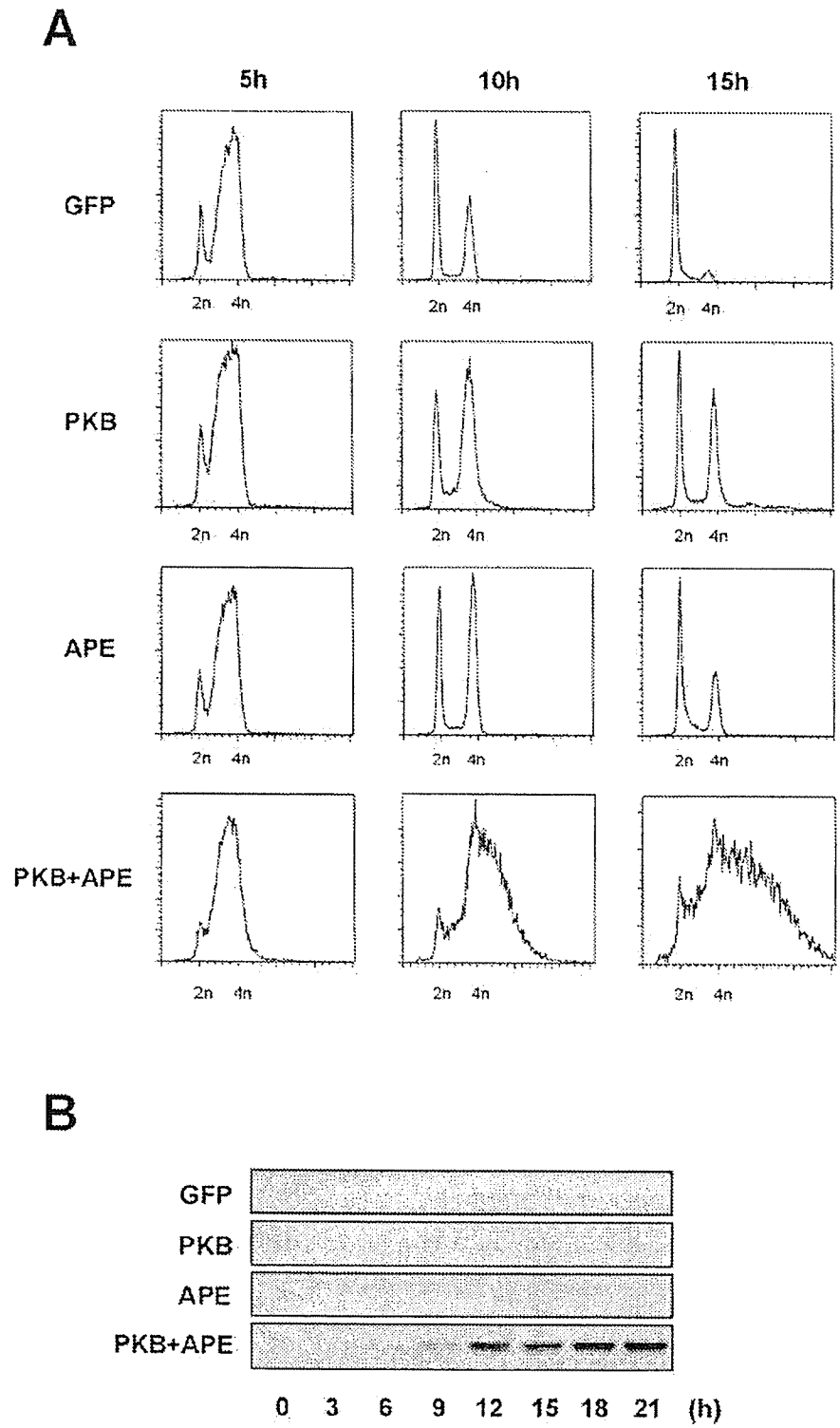

FIG. 9. **Overexpressions of PKBα and APE result in cells with greater than 4n DNA content.** *A*, APE and PKB, alone or in combination, were expressed with an adenovirus expression system, 18 h prior to thymidine release. Cells were collected at the indicated time points after thymidine release. As a control, cells expressing GFP were used. The DNA content was analyzed by fluorescence-activated cell sorting analysis. *2n* (diploid) and *4n* (tetraploid) represent the cells containing 2n and 4n DNA content, respectively. *B*, APE plus PKBα induces phosphorylation of Thr^{68} of Chk2. HeLa cells arrested in G_1/S by a double-thymidine method were released into a synchronous cell cycle and sampled every 3 h. Phosphorylation of Chk2 was determined by immunoblotting with a specific antibody for phospho-Thr^{68} of Chk2.

cells were treated with 1 μM staurosporine, cleaved caspase-3 and cleaved PARP were detectable after 3–6 h, in a time-dependent manner. In COS-7 cells expressing GFP, PKBα, or APE, using an adenovirus expression system, no cleavage of caspase-3 or PARP was detectable. However, in cells expressing both PKBα and APE, cleaved caspase-3 and PARP were

detected. These findings indicate that apoptosis is not induced by PKB alone but rather by the interaction between PKB and APE accompanying prolonged activation of PKBα.

Effect of APE-PKB Interaction on the Cell Cycle—To study the effect of the APE-PKB interaction on cell cycle progression, cell cycle profiles were analyzed using flow cytometry (Fig. 9*A*). Overexpression of PKB or APE alone did not promote rereplication. However, co-expression of PKB and APE generated cells that had DNA contents greater than normal G_2/M cells from 5 to 15 h after thymidine release, indicating that PKB and APE interact to induce DNA rereplication without mitosis.

APE-PKB Interaction Induces Chk2 Phosphorylation—Rereplication reportedly leads to DNA damage, and Vaziri *et al.* (29) demonstrated Chk2 phosphorylation in mammalian cells in which rereplication had been induced by overexpression of the replication license factors CDT1 and CDC6. The amount of Chk2 protein was not altered by PKBα or APE expression (data not shown). However, in HeLa cells overexpressing both PKBα and APE, Chk2 was apparently phosphorylated starting 6 h after thymidine block release, and peak phosphorylation was observed 12–21 h thereafter (Fig. 9*B*). In contrast, overexpression of neither PKBα nor APE induced apparent Chk2 phosphorylation.

DISCUSSION

In this study, we identified a novel PKB-binding protein using a yeast two-hybrid screening system and named it APE. The APE protein was detectable in many tissues including the brain, spleen, lung, fat, and heart, although APE mRNA was most abundant in the testis. In addition, from the immunoblotting results obtained using antibodies against different portions of APE, the presence of alternatively spliced protein products is likely.

The *in vivo* interaction of APE with PKB was clearly demonstrated by the overexpression of both proteins as well as by coimmunoprecipitation of the endogenous proteins. *In vitro* association was also demonstrated using bacterially expressed recombinant proteins. Notably, APE did not interact with any of the other AGC kinases tested in this study such as SGK1/2, PKCβ2, and PKCε, which have regions highly homologous to the hydrophobic motif of PKB. Thus, it is reasonable to consider APE a PKB-specific binding protein.

Subsequently, by overexpressing APE, we demonstrated that this protein markedly enhances the phosphorylation and kinase activity of PKB, whereas reducing endogenous APE expression using siRNA suppressed both. In addition, although APE binds to both phosphorylated and nonphosphorylated PKB, it seems that more PKB binds to APE when PKB is nonphosphorylated. Taking into consideration that APE-induced phosphorylation of PKB did not occur in cells treated with wortmannin or LY294002, APE itself is not a kinase and it is likely that APE enhances or prolongs the PI 3-kinase-dependent phosphorylation of PKB. In other words, we speculate that APE functions as a scaffold protein and facilitates Thr^{308} and Ser^{473} phosphorylation of PKB by PDK1/2. Alternatively, the APE·PKB complex may inhibit access of serine/threonine phosphatases such as protein phosphatase 2A.

Recent evidence indicates that PI 3-kinase and PKB play important roles in regulating cell proliferation. In this study, it was demonstrated that suppression of APE by siRNA reduced DNA synthesis, with decreased phosphorylation and kinase activity of PKB. This result agrees with those of previous reports showing the important role of PKB in proliferation. Thus, when the level of PKB expression is limited, APE apparently enhances proliferation in cooperation with PKB.

On the other hand, interestingly, we demonstrated overexpressions of both APE and PKB to induce DNA rereplication rather than normal DNA synthesis, thereby proving that these overexpressions together increase the cellular DNA content more than 4n in the S phase within 10 h after initiation of the S phase. Similar rereplication was reported with overexpression of the DNA replication factors Cdt1 and Cdc6 in either yeast or mammalian cells (29). In such cell systems, rereplication induced DNA damage, and the checkpoint pathway including Chk2 was activated. Chk2 activation is involved in the p53-dependent apoptotic response observed with DNA damage (30). In good agreement with these previous reports, we observed Chk2 phosphorylation and subsequent apoptosis in PKB and APE-expressing cells, after DNA rereplication. Thus, although the overexpression of both APE and PKB observed in this study may not be physiological, it is likely that the prolonged PKB phosphorylation induced by the association with APE does not lead to normal cell proliferation but rather to rereplication and the ensuing apoptosis. In other words, in the cells with high PKB expression, increased APE expression could lead to apoptosis after DNA rereplication.

Although we cannot explain how PKB and APE induce rereplication in human cells, we observed APE-induced PKB phosphorylation to be markedly enhanced not only in the cytoplasm but also the nucleus (data not shown). Thus, we speculate that overexpressed PKB and APE might phosphorylate some unidentified proteins in the nucleus such that normal replication licensing is blunted. However, this phenomenon was observed only with the overexpression system, and further study is needed to clarify whether this phenomenon is physiological.

In summary, we identified a novel PKB-binding protein, which enhances the phosphorylation of PKB and termed it APE. APE plays a role in regulating the phosphorylation state of PKB and the resultant DNA synthesis. In addition, DNA rereplication and the resultant apoptosis might be a novel mechanism that is induced by the enhanced interaction between APE and PKB, the physiological significance of which merits further investigation.

Acknowledgments—We thank K. Shibata and M. Hirano-Koyanagi for helpful discussions and technical assistance; T. Sugano, T. Kobayashi, M. Mimura, Y. Ito, and other laboratory members for technical assistance and K. Honjo for secretarial assistance.

REFERENCES

1. Lawlor, M. A., and Alessi, D. R. (2001) *J. Cell Sci.* **114,** 2903–2910
2. Datta, S. R., Brunet, A., and Greenberg, M. E. (1999) *Genes Dev.* **13,** 2905–2927
3. Walker, K. S., Deak, M., Paterson, A., Hudson, K., Cohen, P., and Alessi, D. R. (1998) *Biochem. J.* **331,** 299–308
4. Alessi, D. R., Caudwell, F. B., Andjelkovic, M., Hemmings, B. A., and Cohen, P. (1996) *FEBS Lett.* **399,** 333–338
5. Zhou, B. P., Liao, Y., Xia, W., Zou, Y., Spohn, B., and Hung, M. C. (2001) *Nat. Cell Biol.* **3,** 973–982
6. Zhou, B. P., Liao, Y., Xia, W., Spohn, B., Lee, M. H., and Hung, M. C. (2001) *Nat. Cell Biol.* **3,** 245–252
7. Inoki, K., Li, Y., Zhu, T., Wu, J., and Guan, K. L. (2002) *Nat. Cell Biol.* **4,** 648–657
8. Potter, C. J., Pedraza, L. G., and Xu, T. (2002) *Nat. Cell Biol.* **4,** 658–665
9. Pekarsky, Y., Koval, A., Hallas, C., Bichi, R., Tresini, M., Malstrom, S., Russo, G., Tsichlis, P., and Croce, C. M. (2000) *Proc. Natl. Acad. Sci. U. S. A.* **97,** 3028–3033
10. Basso, A. D., Solit, D. B., Chiosis, G., Giri, B., Tsichlis, P., and Rosen, N. (2002) *J. Biol. Chem.* **277,** 39858–39866
11. Maira, S. M., Galetic, I., Brazil, D. P., Kaech, S., Ingley, E., Thelen, M., and Hemmings, B. A. (2001) *Science* **294,** 374–380
12. Du, K., Herzig, S., Kulkarni, R. N., and Montminy, M. (2003) *Science* **300,** 1574–1577
13. Iynedjian, P. B. (2004) *Biochem. J.* **386,** 113–118
14. Yamada, T., Katagiri, H., Asano, T., Inukai, K., Tsuru, M., Kodama, T., Kikuchi, M., and Oka, Y. (2001) *J. Biol. Chem.* **276,** 5339–5345
15. Kamikubo, Y., Takaori-Kondo, A., Uchiyama, T., and Hori, T. (2003) *J. Biol. Chem.* **278,** 17609–17614
16. Downward, J. (1998) *Curr. Opin. Cell Biol.* **10,** 262–267
17. Cross, D. A., Alessi, D. R., Cohen, P., Andjelkovich, M., and Hemmings, B. A. (1995) *Nature* **378,** 785–789
18. Andjelkovic, M., Alessi, D. R., Meier, R., Fernandez, A., Lamb, N. J., Frech, M., Cron, P., Cohen, P., Lucocq, J. M., and Hemmings, B. A. (1997) *J. Biol. Chem.* **272,** 31515–31524
19. Alessi, D. R., Andjelkovic, M., Caudwell, B., Cron, P., Morrice, N., Cohen, P., and Hemmings, B. A. (1996) *EMBO J.* **15,** 6541–6551

20. Stokoe, D., Stephens, L. R., Copeland, T., Gaffney, P. R., Reese, C. B., Painter, G. F., Holmes, A. B., McCormick, F., and Hawkins, P. T. (1997) *Science* **277,** 567–570
21. Stephens, L., Anderson, K., Stokoe, D., Erdjument-Bromage, H., Painter, G. F., Holmes, A. B., Gaffney, P. R., Reese, C. B., McCormick, F., Tempst, P., Coadwell, J., and Hawkins, P. T. (1998) *Science* **279,** 710–714
22. Nakae, J., Park, B. C., and Accili, D. (1999) *J. Biol. Chem.* **274,** 15982–15985
23. Klippel, A., Escobedo, M. A., Wachowicz, M. S., Apell, G., Brown, T. W., Giedlin, M. A., Kavanaugh, W. M., and Williams, L. T. (1998) *Mol. Cell. Biol.* **18,** 5699–5711
24. Kops, G. J., Medema, R. H., Glassford, J., Essers, M. A., Dijkers, P. F., Coffer, P. J., Lam, E. W., and Burgering, B. M. (2002) *Mol. Cell. Biol.* **22,** 2025–2036
25. Dudek, H., Datta, S. R., Franke, T. F., Birnbaum, M. J., Yao, R., Cooper, G. M., Segal, R. A., Kaplan, D. R., and Greenberg, M. E. (1997) *Science* **275,** 661–665
26. Alvarez, B., Martinez, A. C., Burgering, B. M., and Carrera, A. C. (2001) *Nature* **413,** 744–747
27. Oliver, F. J., de la Rubia, G., Rolli, V., Ruiz-Ruiz, M. C., de Murcia, G., and Murcia, J. M. (1998) *J. Biol. Chem.* **273,** 33533–33539
28. Nicholson, D. W., Ali, A., Thornberry, N. A., Vaillancourt, J. P., Ding, C. K., Gallant, M., Gareau, Y., Griffin, P. R., Labelle, M., Lazebnik, Y. A., Munday, N. A., Raju, S. M., Smulson, M. E., Yamin, T. T., Yu, V. L., and Miller, D. K. (1995) *Nature* **376,** 37–43
29. Vaziri, C., Saxena, S., Jeon, Y., Lee, C., Murata, K., Machida, Y., Wagle, N., Hwang, D. S., and Dutta, A. (2003) *Mol. Cell* **11,** 997–1008
30. Jack, M. T., Woo, R. A., Hirao, A., Cheung, A., Mak, T. W., and Lee, P. W. (2002) *Proc. Natl. Acad. Sci. U. S. A.* **99,** 9825–9829

Available online at www.sciencedirect.com
SCIENCE DIRECT
ELSEVIER
Diabetes Research and Clinical Practice 69 (2005) 287–292
DIABETES RESEARCH AND CLINICAL PRACTICE
www.elsevier.com/locate/diabres

WRN gene 1367 Arg allele protects against development of type 2 diabetes mellitus

Masashi Hirai [a,*], Susumu Suzuki [a], Yoshinori Hinokio [a], Takahiro Yamada [a], Shinsuke Yoshizumi [a], Chitose Suzuki [a], Jo Satoh [b], Yoshitomo Oka [a]

[a] *Division of Molecular Metabolism and Diabetes, Department of Internal Medicine, Tohoku University Graduate School of Medicine, 2-1 Seiryo-machi, Aoba-ku, Sendai 980-8575, Japan*
[b] *Department of Diabetology and Metabolism, Iwate Medical University, Japan*

Received 10 August 2004; received in revised form 14 January 2005; accepted 28 January 2005
Available online 16 March 2005

Abstract

Werner's syndrome is an autosomal recessive disease caused by mutation of the *WRN* gene, which may lead to DNA repair failure and acceleration of aging. A polymorphism at amino acid 1367 Cys (TTG)/Arg (CTG) reportedly reduces the risk of myocardial infarction in Japanese. We studied the possible involvement of this polymorphism in type 2 diabetes. When polymorphism of the *WRN* gene was analyzed in 272 randomly recruited type 2 diabetic subjects (age 64.5 ± 11.1), we found those with Cys/Arg to be older than those with Cys/Cys ($p = 0.021$) and that the age at diagnosis of diabetes was greater in Cys/Arg than in Cys/Cys subjects ($p = 0.011$). Diabetes-free survival rate over the age, analyzed by Kaplan–Meier method, differed significantly between these two genotype groups ($p = 0.0125$) and the survival curve was shifted to the right in the Cys/Arg group as compared to the Cys/Cys group. No difference in allele frequency was observed between our diabetic ($n = 272$) and non-diabetic subjects ($n = 171$, age 66.0 ± 8.0). These results suggest that the 1367 Arg allele of the *WRN* gene protects against the development of type 2 diabetes mellitus in Japanese.
© 2005 Elsevier Ireland Ltd. All rights reserved.

Keywords: Type 2 diabetes mellitus; Werner's syndrome; *WRN* gene; *WRN* 1367 Cys/Arg polymorphism; Japanese

1. Introduction

Werner's syndrome is an autosomal recessive disease characterized by early onset of age-related diseases including cataracts, atherosclerosis, osteoporosis, and type 2 diabetes mellitus (DM) [1,2]. Positional cloning identified the gene responsible for Werner's syndrome, which was designated *WRN* [3]. *WRN* encodes a protein (WRN) that is a DNA helicase homologous to *E. coli* RecQ. WRN dysfunction is thought to result in DNA repair failure and acceleration of aging. Homozygous *WRN* mutations resulting in truncation of the protein were demonstrated in Werner's syndrome [4]. However, the effects of heterozygous mutations and rather minor genetic variations in *WRN* on common age-related diseases

* Corresponding author. Tel.: +81 22 717 7611; fax: +81 22 717 7612.
E-mail address: mhirai@int3.med.tohoku.ac.jp (M. Hirai).

0168-8227/$ – see front matter © 2005 Elsevier Ireland Ltd. All rights reserved.
doi:10.1016/j.diabres.2005.01.012

have not been clarified. A polymorphism at amino acid 1367 Cys (TTG)/Arg (CTG) of *WRN* is reportedly associated with myocardial infarction [5–7]; the 1367 Arg allele was suggested to play a protective role. In addition, heterozygous mutation is thought to be involved in common age-related disorders via its effects on the aging process [8]. However, the relevance of heterozygous mutations and the 1367 Cys/Arg polymorphism in type 2 diabetes mellitus has not been clarified. Herein we have shown, for the first time, that in randomly recruited diabetic subjects the development of diabetes is delayed in those with the 1367 Arg allele as compared to those without it. These results suggest that the 1367 Arg allele protects against the development of type 2 diabetes mellitus in Japanese.

2. Subjects and methods

2.1. Subjects

Two hundred and seventy two subjects with type 2 diabetes mellitus (male/female: 124/148) were randomly recruited from among patients seen in Tohoku University Hospital. Diabetes was diagnosed according to World Health Organization (WHO) criteria [9]. Subjects who had developed diabetes before age 30 were excluded from this study, since they may have had MODY or some other specific forms of diabetes. The clinical characteristics of all 272 diabetic subjects are shown in the left column of Table 1. Age at the time of this study averaged 64.5 ± 11.1, at diagnosis 48.8 ± 10.5. The age at diagnosis was determined based on medical records. Treatments were diet alone in 47, oral agents in 85 and insulin in 140. We also recruited 171 non-diabetic individuals as control subjects. The controls met one of the following sets of criteria: (1) age more than 50 and normal glucose tolerance by 75 g oral glucose tolerance test (OGTT) (86 subjects) or (2) HbA1c less than 5.6% and age 65 or older (85 subjects). Homeostasis model assessment for insulin resistance (HOMA-R) was calculated using the formula: fasting serum insulin (μU/ml) × fasting plasma glucose (mg/dl)/405. The study protocol was approved by the Tohoku University Institutional Review Board. Informed consent was obtained from all participants.

2.2. Genotype determination by the TaqMan polymerase chain reaction method

The *WRN* gene polymorphism (1367 Cys (TTG)/Arg (CTG)) was determined by the TaqMan probe method. Two dye-labeled probes were used in this allelic discrimination assay, one probe for each allele in the two-allele system. Each probe consists of an oligonucleotide with a 5′-reporter dye and a 3′-quencher dye. FAM (6-carboxy-fluorescein) was

Table 1
Clinical characteristics of all 272 diabetic subjects and their subgroups based on *WRN* 1367 Cys/Arg genotypes

	DM total	*WRN* 1367 genotype in DM		*p*
		Cys/Cys	Cys/Arg	
N (M/F)	272 (124/148)	244 (112/132)	28 (12/16)	0.759[a]
Age (years)	64.5 ± 11.1	63.9 ± 11.1	69.1 ± 10.1	0.021[b]
Age at diagnosis (years)	48.6 ± 10.5	48.0 ± 10.2	53.3 ± 11.8	0.011[b]
Diabetes duration (years)	15.9 ± 9.9	15.9 ± 9.8	15.8 ± 11.5	0.934[b]
BMI (kg/m^2)	23.5 ± 3.5	23.5 ± 3.4	23.6 ± 4.1	0.848[b]
Fasting plasma glucose (mg/dl)	135.3 ± 26.2	135.9 ± 26.8	130.5 ± 20.0	0.277[b]
HbA1c (%)	6.78 ± 1.10	6.82 ± 1.11	6.45 ± 0.91	0.085[b]
Therapy				
Diet	47 (17.3%)	40 (16.4%)	7 (25%)	0.107[a]
Oral agent	85 (31.3%)	81 (33.2%)	4 (14.3%)	
Insulin	140 (51.5%)	123 (50.4%)	17 (60.7%)	

Data are means ± S.D. unless otherwise specified. *p*-values were obtained by comparing the two genotype groups. DM: diabetes mellitus.
[a] Chi square test.
[b] Student's *t*-test.

covalently linked to the 5′-end of the probe for detection of the T allele. TET (tetrachloro-6-carboxy-fluorescein) was covalently linked to the 5′-end of the probe for detection of the C allele. Each of the reporters is quenched by TAMRA (6-carboxyl-*N,N,N′,N′*-tetramethylrhodamine) attached via a linker arm located at the 3′-end of each probe. The probes used in this study were as follows: a T allele-specific probe, 5′-Fam-CTT CAA CCT TCA TGT GAT GTC AAC AA-Tamra-3′, and a C allele-specific probe, 5′-Tet-CTT CAA CCT TCA CGT GAT GTC AAC AA-Tamra-3′. Primers designed for PCR in the flanking region of the C/T polymorphism in *WRN* were: forward, 5′-GCC TAA TCA GAA TGT TAG TTC C-3′; reverse, 5′-CCT CAG TAT TGA TGC CTA CTT C-3′. PCR was performed with PCR7700 (Applied Biosystems, USA). The fluorescence levels of PCR products were also measured using PCR7700.

2.3. Statistical analysis

Frequency analysis was performed with the chi square test. Significance of differences between group means was tested by Student's *t*-test or analysis of covariance (ANCOVA). Diabetes-free survival rate over the age was determined using Kaplan–Meier analysis and the log rank test in subject groups with the 1367 Cys/Arg or the 1367 Cys/Cys genotype. A *p*-value of less than 0.05 was considered statistically significant.

3. Results

Among 272 subjects with type 2 diabetes, 244 (89.7%) had the Cys/Cys genotype and 28 (10.3%) had the Cys/Arg genotype (Table 2). No subjects had Arg/Arg alleles. The genotype distribution in diabetic subjects did not deviate from Hardy–Weinberg equilibrium. Subjects with the Cys/Cys genotype were compared to those with the Cys/Arg genotype. The clinical characteristics of the diabetic subjects according to *WRN* 1367 genotypes are presented in Table 1. Interestingly, age at the time of the study was significantly greater in those with the Cys/Arg genotype (69.1 ± 10.1) than in those with the Cys/Cys genotype (63.9 ± 11.1) ($p < 0.021$). In addition, age at diabetes diagnosis was approximately 5 years greater in subjects with the Cys/Arg genotype (53.3 ± 11.8) than in those with the Cys/Cys genotype (48.0 ± 10.2) ($p < 0.011$).

Table 2
The Cys/Arg genotype distribution and allele frequencies in Japanese type 2 diabetic and non-diabetic control subjects

	DM	Control
n	272	171
Genotype distribution		
Cys/Cys	244 (89.7)	150 (87.7)
Cys/Arg	28 (10.3)	20 (11.7)
Arg/Arg	0 (0)	1 (0.6)
Cys/Arg + Arg/Arg	28 (10.3)	21 (12.3)
Chi square[a]	0.421	
Odds ratio[a]	1.22	
p[a]	0.51	
Allele frequency		
Cys	516 (94.9)	320 (93.6)
Arg	28 (5.1)	22 (6.4)
Chi square	0.65	
Odds ratio	1.27	
p	0.42	

Data are *n* (%), unless otherwise specified. DM: diabetes mellitus.
[a] Comparison between Cys/Cys and Cys/Arg + Arg/Arg.

Consistent with the age at diagnosis of diabetes differing between the two groups, diabetes-free survival rate over the age, depicted by the Kaplan–Meier method, clearly differed ($p = 0.0125$); the diabetes-free survival curve was shifted to the right in the Cys/Arg group as compared to the Cys/Cys group throughout the 30–80 age range (Fig. 1). The proportions of subjects who had become diabetic by age 50 were 50.0% and 60.7% in the Cys/Arg and the Cys/Cys groups, respectively. Similarly, the proportion who were diabetic by age 60, was also greater in the Cys/Cys (86.9%) than in the Cys/Arg (71.4%) group. Other clinical characteristics, such as BMI at the time of the study, did not differ between the two groups.

Among the 171 non-diabetic subjects, 150 (87.7%) were homozygous for the 1367 Cys allele, 20 (11.7%) were heterozygous and one (0.6%) was homozygous for the 1367 Arg allele. There was no deviation from Hardy-Weinberg equilibrium in control subjects. The genotype distribution did not differ significantly between diabetic and non-diabetic subjects (Table 2). The allele frequencies of the Cys allele

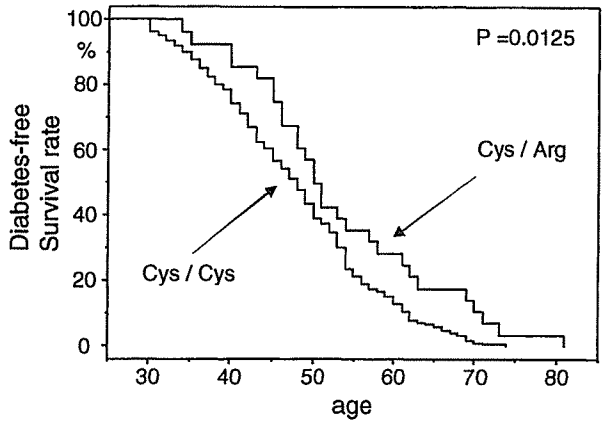

Fig. 1. Diabetes-free survival rate over the age according to the *WRN* 1367 Cys/Arg polymorphism in the diabetic subjects. Kaplan–Meier method.

and the Arg allele were 94.9% and 5.1%, respectively, in diabetic subjects and 93.6% and 6.4%, respectively, in control subjects. There was no statistically significant difference in allele frequencies between these groups.

Eighty-six out of 171 control subjects underwent OGTT to confirm their normal glucose tolerance, and plasma glucose and insulin levels in fasted and glucose challenged states were measured. Therefore, we analyzed the metabolic phenotypes of these subjects in more detail. The fasting glucose, 2 h glucose, fasting insulin, and 2 h insulin levels did not differ markedly (Table 3). Furthermore, HOMA-R (the index of insulin resistance) did not differ before ($p = 0.503$) and after ($p = 0.532$) adjustment for age, gender and BMI.

4. Discussion

Aging has a major influence on glucose intolerance. Werner's syndrome is highly associated with age-related diseases including cataracts, atherosclerosis, osteoporosis, and type 2 diabetes mellitus [1,2]. Thus, *WRN* is a reasonable candidate gene for type 2 diabetes mellitus susceptibility. Herein, we found the current age of diabetic patients with the 1367 Arg allele to be greater than that of those without this allele. In addition, subjects with the 1367 Arg allele develop diabetes later in life than those without this allele. These results suggest that the 1367 Arg allele plays a protective role against the development of diabetes mellitus. Our results might be suggested to simply reflect subjects with the Cys/Cys genotype dying at a younger age, regardless of diabetes. However, this is not the case. The current age of control subjects did not differ between those with (64.4 ± 9.3) and those without (66.2 ± 8.8) the Arg allele. This result may support the notion that subjects without the 1367 Arg allele are more likely to develop diabetes at a younger age than those with this allele, and younger patients are therefore more likely to be recruited into the Cys/Cys group. The following consideration should be reminded in the interpretation of the present results. In this study, we employed the age at diagnosis according to medical records rather than the age at diabetes onset, because it is nearly impossible to ascertain the exact onset of type 2 diabetes in this type of cross-sectional study. Diagnosis of diabetes at a clinical visit may reflect

Table 3
Clinical characteristics according to *WRN* 1367 Cys/Arg genotypes in the control subjects who underwent oral glucose tolerance test

	WRN 1367 genotype in control subjects with OGTT		*p*
	Cys/Cys	Cys/Arg	
N (M/F)	75 (47/28)	11 (9/2)	0.213[a]
Age (years)	59.8 ± 3.5	58.5 ± 2.9	0.232[b]
BMI (kg/m^2)	23.7 ± 2.6	23.2 ± 2.2	0.539[b]
Fasting plasma glucose (mg/dl)	90.7 ± 7.2	91.3 ± 8.0	0.801[b]
2 h plasma glucose (mg/dl)	105.1 ± 19.8	105.6 ± 27.4	0.934[b]
Fasting plasma insulin (μU/ml)	4.36 ± 2.76 ($n = 72$)	3.76 ± 1.89	0.492[b]
2 h plasma insulin (μU/ml)	27.55 ± 19.09 ($n = 71$)	27.61 ± 18.84 ($n = 9$)	0.993[b]
HOMA-R	0.99 ± 0.66 ($n = 72$)	0.85 ± 0.45	0.503[b]

Data are means ± S.D. *p*-values were obtained by comparing the two genotype groups. As complete clinical data were not available for all study subjects, the number of individuals is given in parentheses. OGTT: oral glucose tolerance test.

[a] Chi square test.

[b] Student's *t*-test.

the manifestation of diabetes related symptoms, thus the association of age at diagnosis with *WRN* genotype suggests that this polymorphism influences diabetes development.

Allele frequencies of this polymorphism do not differ between diabetic and non-diabetic subjects. It could be argued that these results are inconsistent with the notion that the 1367 Arg allele protects against the development of diabetes mellitus, as one would expect a higher frequency of the 1367 Arg allele in non-diabetic than in diabetic subjects. This argument is theoretically plausible. However, considering that only a fraction of the general population becomes diabetic and that the effect of the polymorphism is only to delay the onset of diabetes, the allele frequency difference between the diabetic and non-diabetic groups would presumably be very small. Our sample size was large enough to yield 80% power to detect a 5% deviation in the allele frequency between diabetic and control subjects (i.e. 5% in one group and 10% in the other) at a significance level of 0.05. However, the difference in the allele frequency was found to be smaller (5.1% versus 6.4%). Therefore, our results do not rule out the possibility of a slight but significant difference in allele frequency between the two groups, which could not be detected with a sample of this size.

One would expect non-diabetic subjects with the Arg 1367 allele to have slightly lower plasma glucose levels, but this was not the case. All clinical parameters measured, including fasting plasma glucose levels, were the same in subjects with the 1367 Cys allele and those with the 1367 Arg allele. Furthermore, although Werner's syndrome is characterized by insulin resistance, there was no evidence that the *WRN* 1367 polymorphism affected insulin sensitivity judging from the HOMA-R index data (Table 3).

The molecular basis of this polymorphism's contribution to the altered function of the WRN protein has yet to be fully defined. However, sequence analysis and studies using recombinant WRN protein and cells from Werner's syndrome patients have provided interesting findings. The 1367 Cys/Arg polymorphism is located three amino acids from the nuclear localization signal which contains multiple Arg and Lys residues [10,11]. An additional Arg residue near this domain could therefore enhance the rate of intracellular translocation towards the nucleus, thereby enhancing DNA repair capacity. DNA damage occurs with aging and may disturb many physiological functions including glucose metabolism. It is possible that subjects with the 1367 Arg allele are resistant to DNA damage and thus resistant to age-associated glucose intolerance. Further studies are needed to elucidate the roles of the 1367 polymorphism of *WRN* in the aging process and glucose metabolism.

In conclusion, the gene responsible for Werner's syndrome is also involved in the development of a common age-related disorder, diabetes mellitus. Furthermore, the 1367 Arg allele of this gene protects against the development of type 2 diabetes mellitus, delaying diabetes onset in Japanese subjects.

Acknowledgments

This work was supported by a Grant-in-Aid for Scientific Research on Priority Areas (C) "Medical Genome Science" (13204062 to Y.O.) and a Grant-in-Aid for Scientific Research (C) (14571082 to M.H.) from the Ministry of Education, Culture, Sports, Science and Technology of Japan.

References

[1] C.J. Epstein, G.M. Martin, A.L. Schultz, A.G. Motulsky, Werner's syndrome: a review of its symptomatology, natural history, pathologic features, genetics and relationships to the natural aging process, Medicine 45 (1996) 172–221.

[2] M. Goto, Hierarchical deterioration of body systems in Werner's syndrome: implications for normal aging, Mech. Aging Dev. 98 (1997) 239–254.

[3] C.E. Yu, J. Oshima, Y.H. Fu, E.M. Wijsman, F. Hisama, R. Alisch, et al. Positional cloning of the Werner's syndrome gene, Science 272 (1996) 258–262.

[4] T. Matsumoto, O. Imamura, Y. Yamabe, J. Kuromitsu, Y. Tokutake, A. Shimamoto, et al. Mutation and haplotype analyses of the Werner's syndrome gene based on its genomic structure: genetic epidemiology in the Japanese population, Hum. Genet. 100 (1997) 123–130.

[5] L. Ye, T. Miki, J. Nakura, J. Oshima, K. Kamino, H. Rakugi, et al. Association of a polymorphic variant of the Werner helicase gene with myocardial infarction in a Japanese population, Am. J. Med. Genet. 68 (1997) 494–498.

[6] H. Morita, H. Kurihara, T. Sugiyama, C. Hamada, Y. Yazaki, A polymorphic variant $C^{1367}R$ of the Werner helicase gene and atherosclerotic diseases in the Japanese population, Thromb. Haemost. 82 (1999) 160–161.

[7] E. Castro, S.D. Edland, L. Lee, C.E. Ogburn, S.S. Deeb, G. Grown, et al. Polymorphisms at the Werner locus: II. 1074 Leu/Phe, 1367 Cys/Arg, longevity, and atherosclerosis, Am. J. Med. Genet. 95 (2000) 374–380.
[8] M. Satoh, M. Imai, M. Sugimoto, M. Goto, Y. Furuichi, Prevalence of Werner's syndrome heterozygotes in Japan, Lancet 353 (1999) 1766.
[9] K.G.M.M. Alberti, P.Z. Zimmet, Definition, diagnosis and classification of diabetes mellitus and its complications part 1: Diagnosis and classification of diabetes mellitus. Provisional report of a WHO consultation, Diabet. Med. 15 (1998) 539–553.
[10] T. Matsumoto, A. Shimamoto, M. Goto, Y. Furuichi, Impaired nuclear localization of defective DNA helicases in Werner's syndrome, Nat. Genet. 16 (1997) 335–336.
[11] T. Matsumoto, O. Imamura, M. Goto, Y. Furuichi, Characterization of the nuclear localization signal in the DNA helicase involved in Werner's syndrome, Int. J. Mol. Med. 1 (1998) 71–76.

THE JOURNAL OF BIOLOGICAL CHEMISTRY VOL. 280, NO. 51, pp. 42016–42025, December 23, 2005
© 2005 by The American Society for Biochemistry and Molecular Biology, Inc. Printed in the U.S.A.

Resistin-like Molecule β Activates MAPKs, Suppresses Insulin Signaling in Hepatocytes, and Induces Diabetes, Hyperlipidemia, and Fatty Liver in Transgenic Mice on a High Fat Diet*

Received for publication, March 21, 2005, and in revised form, October 18, 2005 Published, JBC Papers in Press, October 21, 2005, DOI 10.1074/jbc.M503065200

Akifumi Kushiyama[‡], Nobuhiro Shojima[‡], Takehide Ogihara[§], Kouichi Inukai[¶], Hideyuki Sakoda[‡], Midori Fujishiro[‡], Yasushi Fukushima[‡], Motonobu Anai[‖], Hiraku Ono[‖], Nanao Horike[**], Amelia Y. I. Viana[**], Yasunobu Uchijima[**], Koichi Nishiyama[**], Tatsuo Shimosawa[‡], Toshiro Fujita[‡], Hideki Katagiri[§], Yoshitomo Oka[§], Hiroki Kurihara[**], and Tomoichiro Asano[**][1]

From the [‡]Department of Internal Medicine, Graduate School of Medicine, University of Tokyo, 7-3-1 Hongo, Bunkyo-ku, Tokyo 113-8655, the [§]Division of Advanced Therapeutics for Metabolic Diseases, Center for Translational and Advanced Animal Research on Human Diseases, Tohoku University Graduate School of Medicine, 1-1 Seiryo-machi, Sendai, Miyagi 980-8574, the [¶]Division of Endocrinology and Diabetes, Department of Medicine, Saitama Medical School, Morohongo 38, Moroyama, Iruma-gun, Saitama 350-0495, the [‖]Department of Internal Medicine, Institute for Adult Diseases, Asahi Life Foundation, 1-6-1, Marunouchi, Chiyoda-ku, Tokyo 100-0005, and the [**]Department of Physiological Chemistry and Metabolism, Graduate School of Medicine, University of Tokyo, 7-3-1 Hongo, Bunkyo-ku, Tokyo 113-8655, Japan

Resistin and resistin-like molecules (RELMs) are a family of proteins reportedly related to insulin resistance and inflammation. Because the serum concentration and intestinal expression level of RELMβ were elevated in insulin-resistant rodent models, in this study we investigated the effect of RELMβ on insulin signaling and metabolism using transgenic mice and primary cultured hepatocytes. First, transgenic mice with hepatic RELMβ overexpression were shown to exhibit significant hyperglycemia, hyperlipidemia, fatty liver, and pancreatic islet enlargement when fed a high fat diet. Hyperinsulinemic glucose clamp showed a decreased glucose infusion rate due to increased hepatic glucose production. In addition, the expression levels of IRS-1 and IRS-2 proteins as well as the degrees of insulin-induced phosphatidylinositol 3-kinase and Akt activations were attenuated in RELMβ transgenic mice. Similar down-regulations of IRS-1 and IRS-2 proteins were observed in primary cultured hepatocytes chronically treated (for 24 h) with RELMβ, suggesting the insulin resistance-inducing effect of RELMβ to be direct. Furthermore, it was shown that RELMβ acutely and markedly activates ERK and p38, while weakly activating JNK, in primary cultured hepatocytes. This increased basal p38 phosphorylation level was also observed in the livers of RELMβ transgenic mice. In conclusion, RELMβ, a gut-derived hormone, impairs insulin signaling probably via the activations of classic MAPKs, and increased expression of RELMβ may be involved in the pathogenesis of glucose intolerance and hyperlipidemia in some insulin-resistant models. Thus, RELMβ is a potentially useful marker for assessing insulin resistance and may also be a target for future novel anti-diabetic agents.

Insulin resistance is a major cause of type 2 diabetes, and recent studies have revealed many independent mechanisms regulating insulin sensitivity. Among them, much attention has been paid to the roles of secreted proteins in insulin resistance. Resistin (also known as FIZZ3 ADSF, mXCP4, or hXCP1) was identified as a factor that is secreted by adipocytes and causes insulin resistance (1). This finding was supported by not only *in vitro* experiments using cultured cells but also animal experiments, *i.e.* mice with adenoviral resistin expression, infusion of recombinant resistin, the use of neutralizing antibody, or by generating resistin gene knock-out mice (2–6). However, some clinical studies have failed to demonstrate a close relationship between obesity or insulin resistance and the serum resistin concentration in humans (7, 8). Thus, while resistin apparently induces insulin resistance, the involvement of resistin in the pathogenesis of human diabetes and obesity remains unclear.

On the other hand, there are three resistin-related proteins, termed RELMα[2] (resistin-like molecule, FIZZ1, or mXCP2), β (FIZZ2, mXCP3, or hXCP2), and γ (mXCP1) (9). RELMα is expressed in white adipose tissue, the lung, tongue and bone marrow, whereas the expression of RELMβ is strictly limited to the small and large intestines, especially goblet cells. Although RELMγ is expressed in mouse spleen, bone marrow, intestines, and a variety of other tissues, corresponding to each developmental stage depending on CAAT/enhancer-binding protein-ϵ (10), its human homolog has not been identified. These proteins contain a highly conserved cysteine-rich C terminus (Cys-X_{11}-Cys-X_8-Cys-X-Cys-X_2-Cys-X_{10}-Cys-X-Cys-X-Cys-X_9-Cys-Cys) and a signal peptide sequence at their N termini, as observed in resistin. Assuming that they have biological activities similar to that of resistin, these RELMs and resistin are considered to be equally important for the regulation of insulin sensitivity. Indeed, it was reported that injecting mice with either resistin or RELMβ induced insulin resistance (11). In addition, we found the intestinal expression and serum concentration of RELMβ to be increased in insulin resistant models such as high fat fed and *db/db* mice (12). Thus, we speculated that the inflammatory state of the intestine, overeating, bowel movements, and/or nutrient absorption might regulate the intestinal expression and serum level of RELMβ and thereby regulate whole-body insulin sensitivity.

* The costs of publication of this article were defrayed in part by the payment of page charges. This article must therefore be hereby marked "*advertisement*" in accordance with 18 U.S.C. Section 1734 solely to indicate this fact.

[1] To whom correspondence should be addressed. Tel.: 81-3-5841-3603; Fax: 81-3-5803-1874; E-mail: asano-tky@umin.ac.jp.

[2] The abbreviations used are: RELM, resistin-like molecule; MAPK, mitogen-activate protein kinase; IRS, insulin receptor substrate; SAPK, stress-activated protein kinase; JNK, c-Jun N-terminal kinase; 2DG, 2-deoxy-D-glucose; PI, phosphatidylinositol; SAP, serum amyloid P; PPARα, peroxisome proliferator-activated receptor α.

Herein, to examine chronic effects of the elevated serum RELMβ observed under insulin-resistant conditions such as a high fat diet and in *db/db* mice, we generated transgenic mice overexpressing RELMβ and analyzed their metabolic profiles relating to insulin resistance and changes in the insulin signaling pathway. Furthermore, to investigate the physiological significance of elevated serum RELMβ, we investigated the effects of RELMβ on insulin signaling using primary cultured hepatocytes. Herein, we show that RELMβ activates three MAPKs and down-regulates IRS-1/2 proteins and suppresses insulin signaling. Our observations suggest that RELMβ may be a useful marker for assessing insulin resistance associated with obesity and may also serve as a target for future novel anti-diabetic agents.

MATERIALS AND METHODS

Antibodies—The affinity-purified antibodies against RELMβ, insulin receptor substrate (IRS)-1, IRS-2, tyrosine phosphorylation (4G10), and Akt/protein kinase B were prepared as previously described (13). The antibodies against phospho-Ser473 of Akt, phospho-p44/p42, p44/42, phospho-p38 MAPK, p38 MAPK, phospho-SAPK/JNK, and SAPK/JNK were purchased from Cell Signaling Technology.

Preparation of Recombinant RELMβ—Adenoviruses expressing RELMβ were constructed using an Ad Easy kit (Quantum Biotechnology). HEK293 T cells transfected with RELMβ adenovirus produced 50–100 mg/liter RELMβ protein in the medium. Serum-free medium CD293 (Invitrogen) was used to collect the secreted protein from confluent HEK293 T cells for 2 days. The medium was harvested and spun down to remove cells. The medium was then purified and concentrated using a high S column and Biologic LP system (Bio-Rad) as described previously (4). Greater than 95% purity was confirmed by silver staining with a Silver Staining Kit (BEXEL Biotechnology), and quantities were determined by Western blotting, using commercially available recombinant RELMβ (Peprotech) as the standard. The medium of HEK293T cells transfected with β-galactosidase expressing adenovirus was used to prepare a control solution. The pH values of RELMβ and control solution were adjusted to 7.4.

Construction of RELMβ and Generation of Transgenic Mice—The open reading frame of RELMβ was obtained employing PCR based on the previously reported sequence (9). This RELMβ cDNA was cloned into a pAT15-3 vector containing the SAP promoter and rat β-globin intron (Fig. 1*a*), which was used for the generation of RELMβ transgenic mice.

Animals and High Fat Diet—The C57/Bl6 line was used to generate RELMβ transgenic mice. All animal studies were conducted according to the Japanese guidelines for the care and use of experimental animals. All animal experiments were performed after 4-week high fat diet loading, unless otherwise indicated. The high fat diet had, basically, the previously described composition (14), except that the skim was added to the formulation. Food intakes were determined daily for 5 consecutive days. Food was withdrawn 12 h before each experiment.

Immunoblotting of RELMβ—Serum RELMβ concentrations in transgenic mice and their littermates were determined by immunoblotting. Two microliters of serum was boiled in Laemmli sample buffer containing 100 mM dithiothreitol. Samples were subjected to SDS-PAGE, transferred to 0.1-μm pore nitrocellulose, and immunoblotted using anti-RELMβ antibody (1:1000). Proteins were visualized with enhanced chemiluminescence (ECL or ECL plus) and exposed to ECL film (Amersham Biosciences)

Serum Glucose, Lipids, and Hepatic Triglyceride and Glycogen—Blood glucose was measured with a portable blood glucose monitor, Freestyle Kissei (Kissei Pharmaceutical, Japan). The plasma insulin level was determined with an enzymatic immunoassay kit (Amersham Biosciences). Serum triglyceride, cholesterol, and free fatty acids were assayed with Triglyceride E test Wako, Cholesterol E test Wako, and NEFA C test Wako (Wako Chemicals, Japan), respectively. Serum adiponectin was assayed with an adiponectin measurement kit (Otsuka Pharmaceuticals, Japan). Hepatic total lipid was extracted and assayed using the Folch method, as described previously (15). The triglyceride content was assayed as described above. Hepatic glycogen content was measured as previously described (16).

Tolerance Test—Glucose (2 g/kg glucose load), insulin (0.75 unit/kg insulin), and pyruvate (2 g/kg pyruvate) tolerance tests were performed as previously described (17).

Glucose Clamp Study—The glucose clamp study was performed, as previously described (18–21), with some modifications. In brief, mice were implanted with catheters that were exteriorized at the back of the neck and encased in silastic tubing. Four days after surgery, the animals were fasted for 3 h and used for the experiments. [D-^{3}H]Glucose (Amersham Biosciences) was injected (bolus 10 μCi, 0.1 μCi/min, for 240 min) intravenously. After a 90-min basal period, a blood sample was collected for determination of glucose-specific activity and the blood glucose level. At time 0, hyperinsulinemic-euglycemic clamps were started, and 10 milliunits/kg/min human insulin (Novolin R, Novo Nordisk) was continuously infused for 150 min. The blood glucose concentration was clamped at 90–120 mg/dl, for at least 60 min, by estimating the blood glucose concentration at 5-min intervals and adjusting the rate of glucose solution infusion. Blood samples were taken to determine blood glucose, insulin, and plasma [D-^{3}H]glucose every 30 min for 120 min. Then, 12 μCi of [^{14}C]2-deoxy-D-glucose ([^{14}C]2DG, Amersham Biosciences) was injected, and blood samples were taken at 122, 125, 130, and 150 min to determine blood glucose and plasma [^{14}C]2DG. At 150 min, the gastrocnemius (type IIB fibers) muscle, soleus (type I and type IIA fibers) muscles, and epididymal fat were immediately excised and frozen in liquid nitrogen, then stored at −80 °C until future tissue analysis.

Plasma and Tissue Assays in Glucose Clamp Study—After deproteinization with barium hydroxide ($Ba(OH)_2$, 0.3 N) and zinc sulfate ($ZnSO_4$, 0.3 N), [D-^{3}H]glucose and [^{14}C]2DG radioactivities of plasma were determined by dual channeled liquid scintillation counting. Hepatic glucose production and the glucose disposal rate were calculated for the basal period and the steady-state portion of the glucose clamp as previously described (21). Muscle and fat samples were weighed and homogenized in 0.5% perchloric acid. Homogenates were centrifuged and neutralized with $NaHCO_3$. The sample was then separated into two aliquots. One was counted directly to determine [^{14}C]2DG and [^{14}C]2DG-6-phosphate ([^{14}C]2DGP) radioactivities. The other was treated with $Ba(OH)_2$ and $ZnSO_4$ to remove [^{14}C]2DGP and any tracer incorporated into glycogen and then counted to determine [^{14}C]2DG radioactivity. [^{14}C]2DGP is the difference between the two aliquots. Tissue glucose uptake was calculated as described (20).

In Vivo Insulin Stimulation—*In vivo* insulin stimulation was performed, as previously described (22), with some modifications. In brief, mice were anesthetized with pentobarbital sodium. The portal vein was exposed, and 0.4 ml of normal saline (0.9% NaCl) with or without insulin (25 milliunits/g body wt) was injected. The livers were removed 30 s later, and hind limb skeletal muscles were removed 90 s thereafter and immediately homogenized with a Polytron homogenizer in 6 volumes of solubilization buffer. Both extracts were centrifuged at 15,000 × *g* for 30 min at 4 °C, and the supernatants were used as samples for immunoprecipitation, immunoblotting, or kinase assay of PI 3-kinase and Akt/protein kinase B.

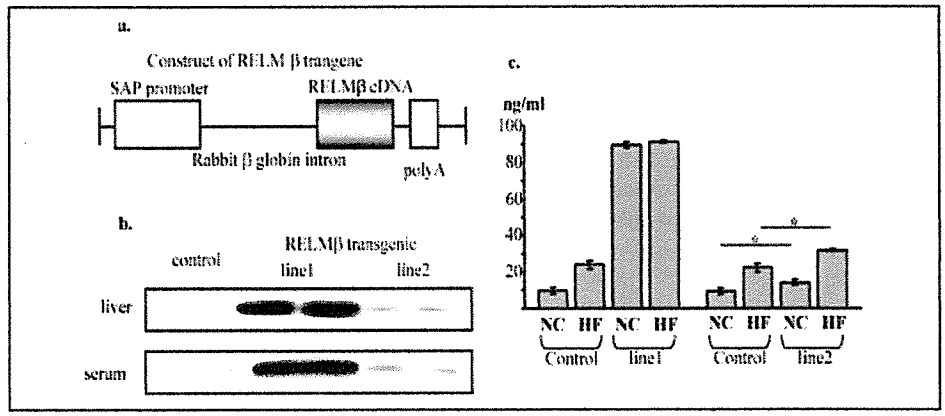

FIGURE 1. *a*, schematic drawing of the construct for RELMβ gene overexpression. *b*, hepatic expressions and elevated serum concentrations of RELMβ in the two lines of RELMβ transgenic mice. Immunoblotting revealed line 1 and line 2 transgenic mice to have high and low levels of RELMβ overexpression, respectively. *c*, quantification using recombinant RELMβ as the standard. Western blotting was performed by transferring samples, using standards for the same membrane. Values are presented as means ± S.E. In line 2 mice, statistical significance is indicated by an *asterisk*: *, $p < 0.05$ for RELMβ transgenic mice *versus* control age-matched mice. *NC*, normal chow; *HF*, high fat.

Immunoprecipitation and Immunoblotting—Supernatants containing equal amounts of protein (8 mg) were incubated with anti-IRS-1 and anti-IRS-2 antibodies (5 mg/ml each) and then incubated with 100 μl of protein A- and G-Sepharose. The samples were washed and then boiled in Laemmli sample buffer containing 100 mM dithiothreitol. Total lysates were also boiled to allow detection of Akt, AktSer473 phosphorylation, the three MAPKs, and their phosphorylations. Total lysates or immunoprecipitants were subjected to Western blotting, blotted with one of the antibodies or 4G10 antibody. Band intensities were quantified with Image J (National Institutes of Health).

Measurement of PI 3-Kinase and Akt/Protein Kinase B Activity—For PI 3-kinase assay, the supernatants containing equal amounts of protein were immunoprecipitated for 2 h at 4 °C with anti-IRS-1, anti-IRS-2 or 4G10 antibody and protein A- or G-Sepharose. PI 3-kinase activities in the immunoprecipitants were assayed as previously described (23). For the Akt kinase assay, an Akt kinase assay kit (Cell signaling) was used according to the manufacturer's instructions.

Glucose Uptake by Isolated Soleus Muscle in Vitro—Insulin-stimulated glucose uptake by the soleus muscle was measured as described previously (24). Mouse soleus muscles were isolated and incubated for 30 min in KHB buffer, with or without human insulin (2 milliunits/ml). The muscles were then rinsed for 10 min at 29 °C and incubated for 20 min at 29 °C in KHB buffer containing 8 mM 2-deoxy-D-[1,2-^{3}H]glucose (2-DG) (2.25 μCi/ml) and 32 mM [^{14}C]mannitol (0.3 μCi/ml). After incubation, the muscles were rapidly solubilized. Radioactivity in the resultant samples was counted, and 2-DG uptake rates were corrected for extracellular trapping with mannitol counts.

Effects of RELMβ on Insulin Action in Primary Hepatocytes—Hepatocytes were isolated from fasted C57/bl6 mice by collagenase perfusion, as described previously (25). To determine the effects of RELMβ on insulin signaling, the dishes were split into two groups corresponding the presence and absence of RELMβ stimulation for 24 h. The RELMβ concentration was 1 μg/ml. The cells were then serum-starved for 3 h and stimulated with 10^{-6} M insulin for 5 min at 37 °C. IRS-1 and IRS-2 protein contents were evaluated by immunoblotting as described above. Insulin-induced IRS-1 and IRS-2 phosphorylations were evaluated by 4G10 immunoprecipitation and immunoblotting as described above.

Effect of RELMβ on Phosphorylations of MAPKs—To determine the effects of RELMβ on MAPK phosphorylations with their time course and dose dependence, primary hepatocytes were stimulated with 1 μg/ml RELMβ for 10 or 30 min, and with 0.01, 0.1, or 1 μg/ml RELMβ for 15 min. Phosphorylations of p44/p42 (ERK1/2), p38 MAPK, and p54/p46 (SAPK/JNK) were evaluated by immunoblotting as described previously (26).

Tissue Hematoxylin-Eosin Staining—The liver and pancreas were removed from transgenic mice and their littermates and formalin-fixed. Samples were routinely embedded in paraffin. Approximately 5-μm-thick slices obtained from these samples were stained with hematoxylin and eosin. Mean pancreatic islet area was histomorphometrically analyzed as previously described (27), using ImageJ (National Institutes of Health).

Ribonuclease Protection Assay—Riboprobes of enzymes were amplified from mouse embryonic cDNA using PCR primers and subcloned as already described (13). Total RNA from the liver and primary cultured hepatocytes was isolated using TRIzol reagent (Isogen, Nippon Gene, Japan). A 10-μg RNA sample was used for each assay. RNase protection assays were carried out according to the manufacturer's instructions (RPA III kit, Ambion, Austin, TX). Intensities of the resultant bands were determined using BAS2000 (Fuji film, Japan).

Statistical Analysis—Results are expressed as means ± S.E., and significance was assessed using unpaired Student's *t* tests, unless otherwise indicated.

RESULTS

Generating RELMβ Transgenic Mice—We generated transgenic mice, the livers of which express RELMβ, by inserting RELMβ cDNA downstream from the serum amyloid P (SAP) promoter. As expected, liver-specific expression in these transgenic mice was confirmed (data not shown), and two lines were established. In the livers of line 1 mice, RELMβ was highly overexpressed, and the serum RELMβ concentration exceeded that of the non-transgenic mice by 10-fold (Fig. 1*c*). In line 2 mice, RELMβ was moderately overexpressed, and the resulting elevation of serum RELMβ was approximately double that in non-transgenic mice (Fig. 1*c*). Hepatic RELMβ expression was reportedly increased in response to high fat feeding. Thus, increases in serum RELMβ with a high fat diet were observed in wild-type and line 2 mice, whereas there was no marked increase in the line 1 mice in which hepatic RELMβ overexpression was high. These observations indicate that a high fat diet increases endogenous RELMβ expression but not transgene-derived RELMβ expression.

No significant difference was observed in terms of growth or adolescence between RELMβ transgenic mice and their littermates. At the time of sacrifice (age 16 weeks, after 4 weeks of being fed a high fat diet) and within the observation period, there was no significant difference in body weight or food intake.

Glucose and Lipid Metabolic Profiles of RELMβ Transgenic Mice—The body weight, fasting serum glucose, serum insulin, and lipid concentrations of RELMβ transgenic mice did not differ from those of control mice when both were fed normal chow, at the age of 16 weeks.

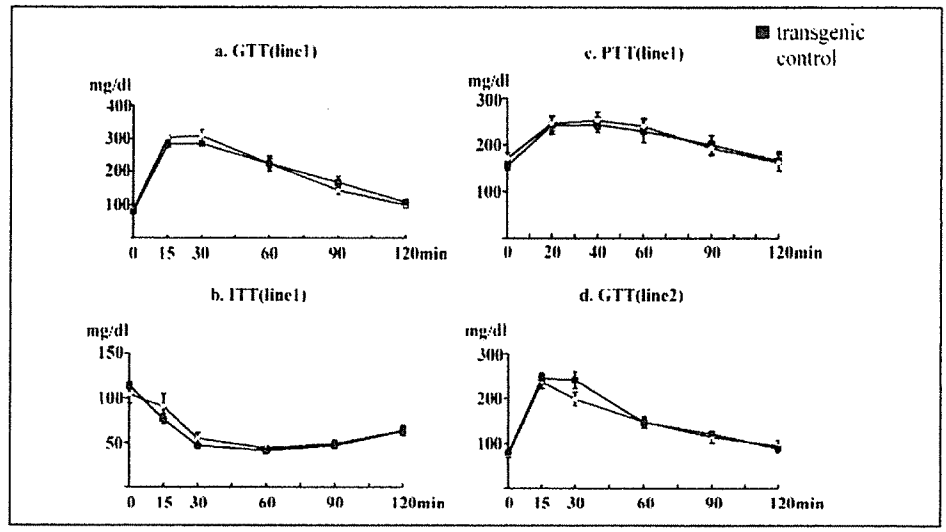

FIGURE 2. **Intraperitoneal glucose tolerance test (GTT), insulin tolerance test (ITT), and pyruvate tolerance test (PTT) in age-matched RELMβ transgenic (■, $n = 6$ for line 1 and $n = 5$ for line 2) and control mice (○, $n = 7$ for line 1 and $n = 8$ for line 2).** *a* and *d*, GTT for line 1 (age 6 weeks, normal chow) and 2 (age 6 weeks, normal chow) in comparison with the control mice. *b*, ITT for line 1 (age 7 weeks, normal chow) in comparison with the control mice. *c*, PTT for line 1 (age 8 weeks, normal chow) in comparison with the control mice. Values are presented as means ± S.E.

TABLE ONE

Glucose and lipid metabolic profiles of 16-week-old RELMβ transgenic mice on normal chow

Values are indicated as means ± S.E. *TC*, total cholesterol; *TG*, triglyceride.

	Control (line 1)	Transgenic (line 1)	Control (line 2)	Transgenic (line 2)
BW (g)	17.2 ± 0.8	17.9 ± 0.5	15.4 ± 1.1	16.4 ± 0.6
FBS (mg/dl)	88.9 ± 4.1	92.0 ± 2.4	81.2 ± 2.7	86.8 ± 2.6
Serum insulin (ng/ml)	0.08 ± 0.02	0.11 ± 0.02		
Serum TC (mg/dl)	38.2 ± 2.2	36.7 ± 3.3		
Serum TG (mg/dl)	49.6 ± 8.1	49.0 ± 5.8		
Serum free fatty acid (mEq/liter)	0.80 ± 0.08	0.63 ± 0.07		

TABLE TWO

Glucose and lipid metabolic profiles of RELMβ transgenic mice, at the age of 16 weeks, which had been fed a high fat diet for 4 weeks

Values are indicated as means ± S.E. *TC*, total cholesterol; *TG*, triglyceride.

	Control (line 1)	Transgenic (line 1)	Control (line 2)	Transgenic (line 2)
Body weight (g)	37.1 ± 2.6	36.5 ± 1.4	31.5 ± 1.5	33.9 ± 2.6
Food intake (g/day)	4.6 ± 0.4	4.5 ± 0.5	4.1 ± 0.2	4.3 ± 0.8
FBS (mg/dl)	109.5 ± 8.3	156.1 ± 10.6[a]	117.3 ± 3.9	132.0 ± 2.8[a]
Serum insulin (ng/ml)	3.8 ± 0.7	12.3 ± 2.7[a]	5.4 ± 1.3	7.6 ± 1.4
Serum TC (mg/dl)	48.0 ± 3.6	61.2 ± 7.9[a]	50.3 ± 4.5	76.4 ± 13.6
Serum TG (mg/dl)	51.7 ± 6.4	84.6 ± 6.4[a]	75.9 ± 8.0	103.3 ± 14.0[a]
Serum free fatty acid (mEq/l)	0.59 ± 0.02	0.56 ± 0.04	NT[b]	NT
Serum adiponectin (μg/ml)	14.1 ± 1.4	11.1 ± 0.9	NT	NT
Liver TG (mg/g liver)	14.3 ± 1.9	21.0 ± 2.9[a]	NT	NT
Liver glycogen (mg/g liver)	1.96 ± 0.08	1.97 ± 0.10	NT	NT
Islet area (μm^2)	36310 ± 6357	92760 ± 9571[a]	NT	NT

[a] Statistical significance: $p < 0.05$ for control mice *versus* transgenic mice.
[b] NT, not tested.

Furthermore, glucose, insulin, and pyruvate tolerance tests showed no significant differences between 16-week-old RELMβ-overexpressing mice and their littermates (Fig. 2, *a–d*, and TABLE ONE). However, the serum glucose concentration was significantly more elevated in both lines of transgenic mice ($n = 25$, $p < 0.01$) when fed a high fat diet (TABLE TWO), than those in the control mice. Under these conditions, hyperinsulinemia ($n = 6$, $p < 0.05$), hyperlipidemia ($n = 6$, $p < 0.05$), and increased hepatic triglyceride content ($n = 8$, $p < 0.05$) were observed in the transgenic mice.

Starting at the age of 16 weeks (line 1), or 20 weeks (line 2), mice were given a high fat diet for 4–6 weeks, and glucose, insulin, and pyruvate tolerance tests were then performed (Fig. 3). The glucose tolerance test confirmed an elevated fasting serum glucose concentration (Fig. 3, *a* and *d*) and revealed glucose intolerance in the transgenic mice. The insulin tolerance test revealed insulin resistance in the transgenic mice (Fig. 3, *b* and *e*). Finally, the pyruvate tolerance test showed greater elevation of the serum glucose concentration in the transgenic mice, as compared with the control mice (Fig. 3, *c* and *f*), indicating insufficient suppression of hepatic gluconeogenesis in the transgenic mice. Taking these results together, RELMβ transgenic mice are insulin-resistant and glucose-intolerant, particularly in the liver. These tendencies were more evident in the highly RELMβ-overexpressing line. In terms of adipocytokines,

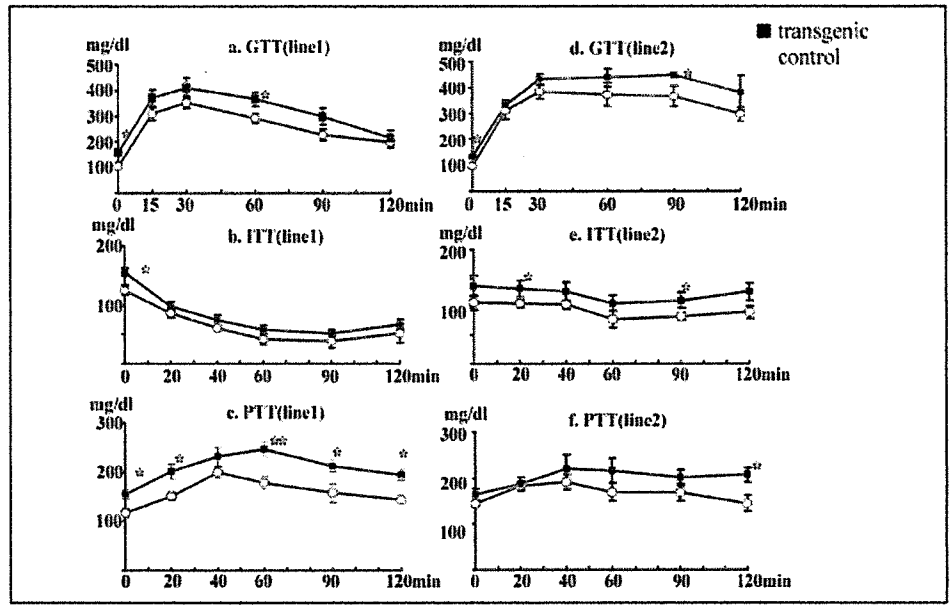

FIGURE 3. **Intraperitoneal glucose tolerance test (GTT), insulin tolerance test (ITT), and pyruvate tolerance test (PTT) in age-matched RELMβ transgenic (■, $n = 8$ for line 1 and $n = 7$ for line 2) and control mice (○, $n = 5$ for line 1 and $n = 7$ for line 2).** *a* and *d*, GTT for line 1 (age 16 weeks, fed a high fat diet for 4 weeks) and 2 (age 20 weeks, fed a high fat diet for 4 weeks) in comparison with the control mice fed a high fat diet for 4 weeks, respectively. *b* and *e*, ITT for line 1 (age 17 weeks, fed a high fat diet for 5 weeks) and 2 (age 21 weeks, fed a high fat diet for 5 weeks) in comparison with the control mice fed a high fat diet for 4 weeks, respectively. *c* and *f*, PTT for line 1 (age 18 weeks, fed a high fat diet for 6 weeks and 2 (age 22 weeks, fed a high fat diet for 6 weeks) in comparison with the control mice fed a high fat diet for 6 weeks, respectively. Values are presented as means ± S.E. Statistical significance is indicated by an *asterisk*: *, $p < 0.05$ for RELMβ transgenic mice *versus* control age-matched mice.

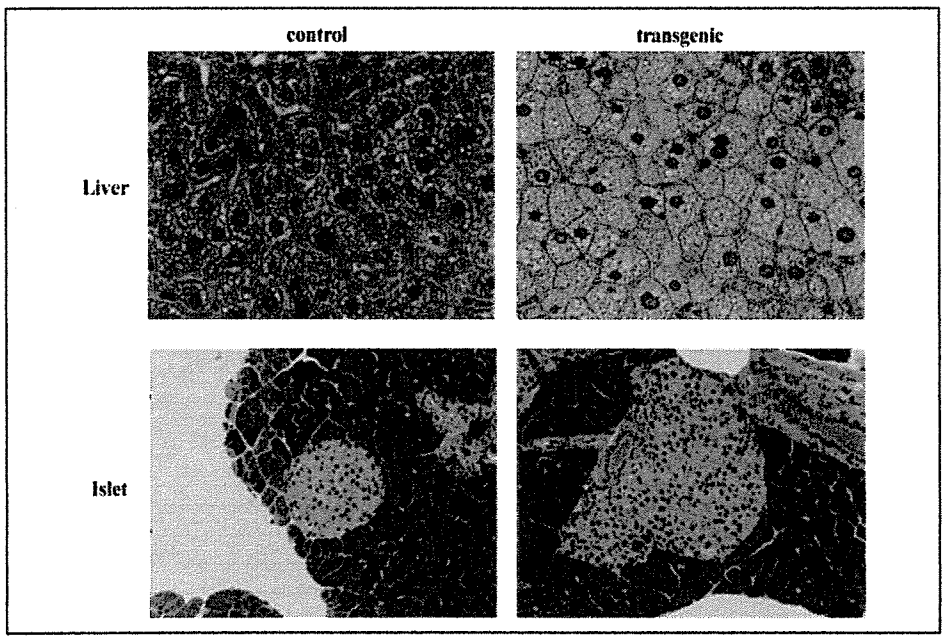

FIGURE 4. **Liver and pancreatic islet histologies in 16-week-old line 1 RELMβ transgenic and control mice that had been fed a high fat diet for 4 weeks.** Liver and pancreatic sections from adult, high fat diet fed mice were stained with hematoxylin and eosin. The mean islet area is presented in TABLE TWO.

the levels of serum free fatty acid and adiponectin were not altered (n = 8–10).

Histological Analysis of Liver and Pancreas—Histology showed fatty liver and islet hyperplasia in transgenic mice as compared with control mice (n = 3, age 16 weeks, after 4 weeks on a high fat diet, Fig. 4). Quantitatively, the mean islet area in RELMβ-overexpressing mice was significantly increased, as compared with that in control mice, by approximately 2.5-fold (TABLE TWO). In contrast, no significant difference in adipocyte size or mass was seen in epididymal or subcutaneous fat at the time of sacrifice (data not shown).

Glucose Clamp Study and Glucose Uptake in Vivo and in Vitro—Six-month-old mice fed a high fat diet for 4 weeks were used for the glucose clamp study. In the basal state, glucose levels were 113.3 ± 2.0 *versus* 158 ± 9.5 mg/dl (control *versus* transgenic), and insulin levels were 5.0 ± 1.2 *versus* 12.1 ± 5.4 ng/ml. There was no significant difference in either glucose utilization or hepatic glucose output (Fig. 5, *b* and *c*). In the hyperinsulinemic euglycemic clamp study, glucose levels were 96.0 ± 5.3 *versus* 100.8 ± 5.3 mg/dl, and insulin levels were 20.3 ± 5.2 *versus* 22.4 ± 2.8 ng/ml. RELMβ transgenic mice showed a 35% lower glucose infusion rate (Fig. 5*a*) due to markedly insufficient suppression of hepatic glucose output, (about one-fifth of the expected suppression, Fig. 5*c*), whereas hyperinsulinemia had no effect on the glucose disappearance rate (Fig. 5*b*).

We found no significant difference in glucose uptake *in vivo* during the clamp by either muscles or fat (Fig. 5*d*), nor in insulin stimulated glucose uptake *in vitro* by isolated soleus muscle between RELMβ-overexpressing mice and their littermates, at 3 months of age after 4 weeks on a high fat diet, *i.e.* immediately before the experiment (Fig. 5*e*).

Insulin Signaling in RELMβ Transgenic Mice—To reveal the mechanism of glucose intolerance in the RELMβ transgenic mice, we investi-

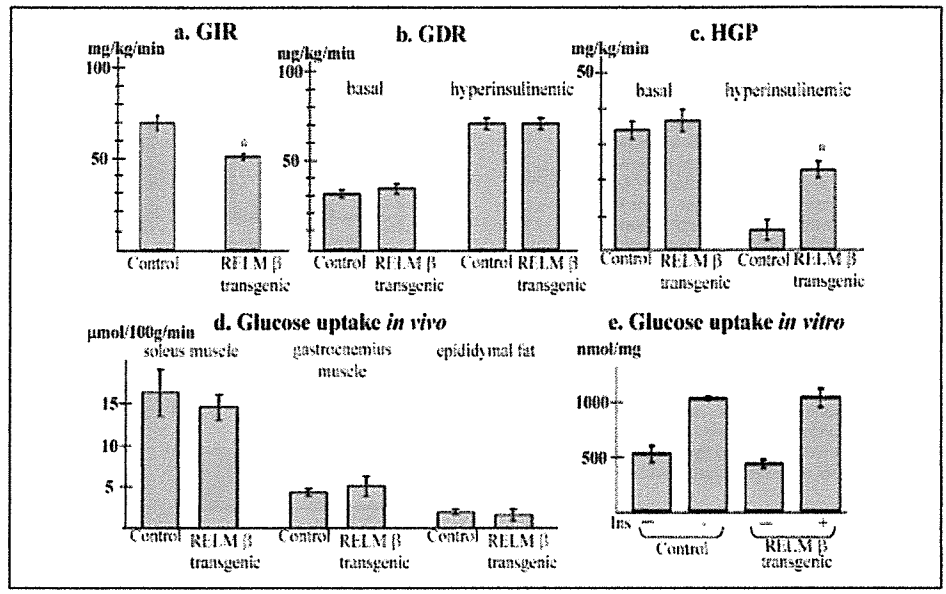

FIGURE 5. *a–d*, glucose clamp study of RELMβ overexpressing line 1 at 6 months of age, following 4 weeks of being fed a high fat diet. Blood samples were collected every 30 min to determine the glucose specific activity and blood glucose and plasma insulin concentration during 90-min basal period and 150-min clamp period. At the end of the study, tissues were sampled for determination of tissue glucose uptake rates during the clamp period. *a*, glucose infusion rate in the hyperinsulinemic euglycemic state. *b*, glucose disposal rates in basal and hyperinsulinemic states. *c*, glucose production rate in basal and hyperinsulinemic states. *d*, glucose uptake by soleus muscle, gastrocnemius muscle, and epididymal fat *in vivo*. *e*, glucose uptake by isolated soleus muscle *in vitro*. −, without insulin stimulation; +, with insulin stimulation. Values are presented as means ± S.E. In *b–e*, statistical analysis was performed using two-way analysis of variance. Statistical significance is indicated by an *asterisk*: *, $p < 0.05$ for RELMβ transgenic mice *versus* control age-matched mice.

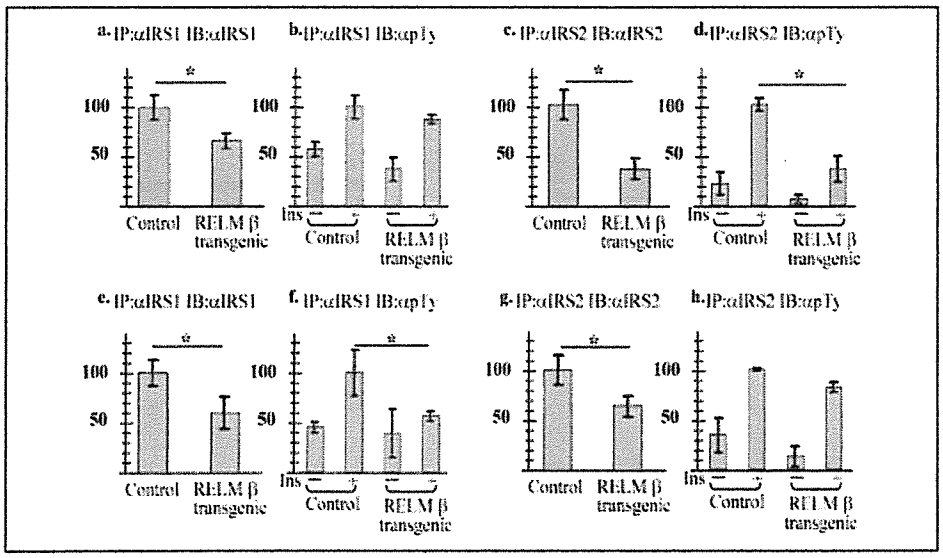

FIGURE 6. **The protein contents and phosphorylations of IRS-1/2 in liver (*a–d*) and muscle (*e–h*) from 3-month-old RELMβ-overexpressing line 1 mice, which had been fed a high fat diet for 4 weeks.** Values are presented as means ± S.E. −, without insulin stimulation; +, with insulin stimulation. The *scale* represents the percentage of control (with insulin stimulation, if performed). Statistical significance is indicated by an *asterisk*: *, $p < 0.05$ for control mice *versus* transgenic mice.

gated protein contents, phosphorylations, and insulin signaling cascade activity using the highly RELMβ-overexpressing (*line 1*, Fig. 1*b*) line 1 3-month old mice, which had been fed a high fat diet for 4 weeks. We found that IRS-1 and IRS-2 protein contents were significantly decreased in the livers and muscles of transgenic mice (IRS-1: 34% decrease in liver, 40% in muscle, $p < 0.05$; IRS-2: 64% in liver and 36% in muscle, $p < 0.05$) (Fig. 6, *a*, *c*, *e*, and *g*). The insulin-induced tyrosine phosphorylations of IRS-1 and IRS-2 were also decreased in the livers and muscles of transgenic mice (Fig. 6, *b*, *d*, *f*, and *h*). In the liver, the decrease in IRS-2 phosphorylation ($p < 0.05$) was more evident than that of IRS-1, whereas the IRS-1 decrease was more evident in muscle. Similarly, the PI 3-kinase activities associated with IRS-1 and IRS-2 in response to insulin stimulation were significantly suppressed, by ~40%, in transgenic mice (Fig. 7, *a–e*). Finally, Akt kinase activity in the presence of insulin stimulation was also decreased in both liver (40%) and muscle (35%) in transgenic mice (Fig. 8, *a–e*), whereas Akt protein contents were not significantly altered.

RELMβ Activates ERK, p38, and JNK while Suppressing Insulin Signaling in Primary Cultured Hepatocytes—To investigate the effects of RELMβ on insulin signaling in the liver, primary cultured hepatocytes were prepared. The treatment of hepatocytes with 1 μg/ml of recombinant RELMβ for 24 h induced apparent decreases in both IRS-1 (70% $p < 0.005$) and IRS-2 (49%, $p < 0.005$) protein contents (Fig. 9, *a* and *b*). Similarly, insulin-stimulated phosphorylations of IRS-1 and IRS-2 were also suppressed by treatment with RELMβ (Fig. 9, *c* and *d*). Subsequently, mRNA levels of gluconeogenetic enzymes, glucose-6-phosphatase, and phosphoenolpyruvate carboxylase kinase were elevated (Fig. 9, *e* and *f*). This suggested RELMβ to directly produce insulin resistance in the liver.

Next, to reveal the molecular mechanism underlying the suppressed expression and phosphorylation of IRS-1 and IRS-2, we studied the effects of RELMβ on the three MAPKs, ERK, p38, and SAPK/JNK, all of which can reportedly induce insulin resistance. Hepatocytes were treated with 1 μg/ml RELMβ or 10 ng/ml tumor necrosis factor α for 10 or 30 min, and the phosphorylations of ERK,

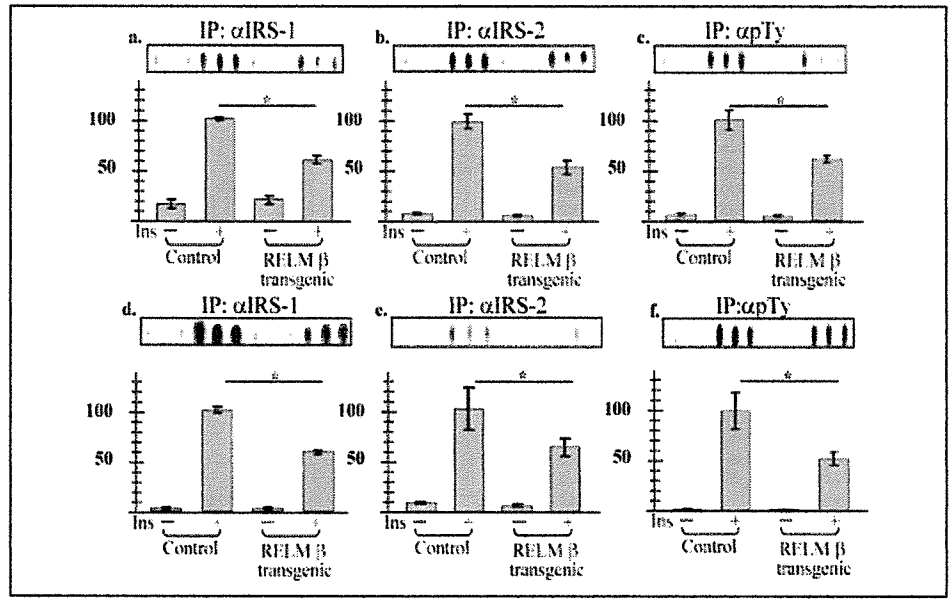

FIGURE 7. **Insulin-induced PI 3-kinase activation in 3-month-old line 1 RELMβ transgenic and control mice that had been fed a high fat diet for 4 weeks.** *a–c*, phosphorylation of PI was carried out in immune complexes from the liver lysate. *a–c*, are IRS-1-, IRS-2-, and pTy-associated PI 3-kinase activities, respectively. *d–f*, phosphorylation of PI was carried out in immune complexes from the muscle lysate. *d–f*, are IRS-1-, IRS-2-, and pTy-associated PI3K activities, respectively. *Lower portions* of the *upper panels* show the autoradiographic results of the PI 3-kinase assay, and means ± S.E. values are presented in the *lower panels*. −, without insulin stimulation; +, with insulin stimulation. The *scale* represents the percentage of control with insulin stimulation. Statistical significance is indicated by an *asterisk*: *, $p <$ 0.05 for control mice *versus* transgenic mice.

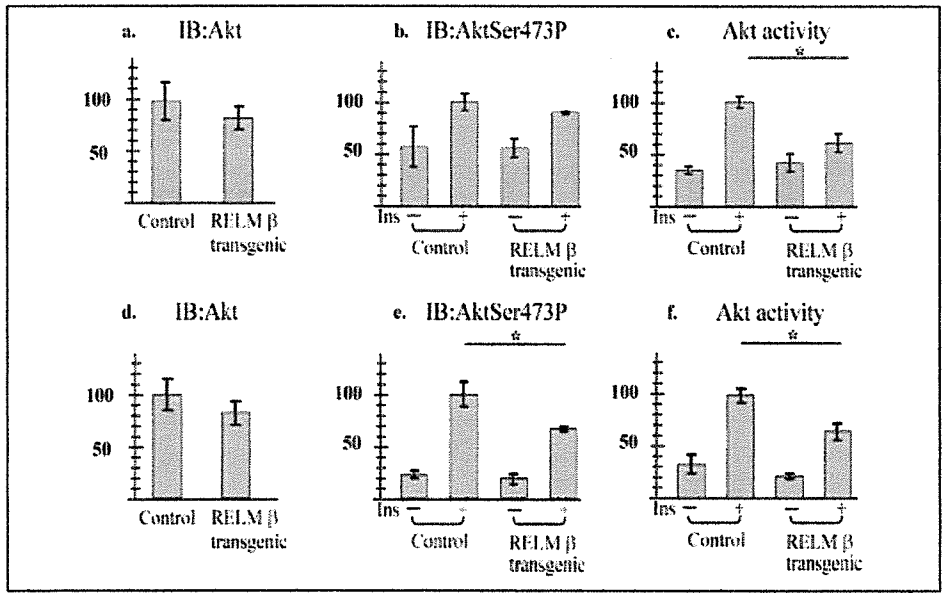

FIGURE 8. **The protein contents, phosphorylation of Akt, and Akt activity in liver (*a–c*) and muscle (*d–f*) from 3-month-old RELMβ-overexpressing line 1 mice, which had been fed a high fat diet for 4 weeks.** Values are presented as means ± S.E. −, without insulin stimulation; +, with insulin stimulation. The *scale* represents the percentage of control (with insulin stimulation, if performed). Statistical significance is indicated by an *asterisk*: *, $p < 0.05$ for control mice *versus* transgenic mice.

p38, and JNK were assessed by immunoblotting with the antibodies to detect phosphorylation of p44/p42 (ERK1/2), p38 MAPK, and p54/p46 (SAPK/JNK). RELMβ was revealed to markedly phosphorylate ERK and p38, but JNK only weakly (*left side* of Fig. 10, *a* and *c*). The phosphorylations induced by RELMβ were more intense 30 min after the initiation of stimulation than at 10 min, whereas tumor necrosis factor α-induced phosphorylations of MAPKs were shown to peak at ~10 min (*right side* of Fig. 10*a*). The effect of RELMβ was concentration-dependent, and as little as 10 ng/ml RELMβ stimulated all three MAPKs (Fig. 10, *b* and *d*). In addition, increased phosphorylation of p38 was observed in both the liver and muscle of RELMβ transgenic mice (Fig 11) in the basal, *i.e.* fasted, state, although there were no significant changes in the phosphorylations of ERK and JNK.

Key Enzymes for Lipid Metabolism Showed Modestly Altered Transcriptional Levels in RELMβ Transgenic Mice—To investigate the mechanisms of hyperlipidemia in RELMβ transgenic mice, mRNA levels of key lipid metabolic enzymes were evaluated using a RELMβ-overexpressing line (*line 1*) *i.e.* 3-month-old mice that had been fed a high fat diet for 4 weeks. A lipogenic enzyme (fatty acid synthase, 60%) was increased and lipolytic enzymes (carnitine palmitoyltransferase-1, 32%, PPARα: peroxisome proliferator activated receptor-α, 33%) were decreased (TABLE THREE). These changes probably contribute to the mechanisms underlying the moderate hyperlipidemia in RELMβ-overexpressing mice.

DISCUSSION

Although the gut is the site of nutrient absorption, the gastrointestinal tract secretes several hormones such as glucagon-like peptide-1, gastric inhibitory polypeptide, and ghrelin. These hormones reportedly influence metabolic conditions by regulating insulin secretion and appetite (28–31). Recently, two RELMs were also identified as hormones secreted from the mouse small intestine and colon (9, 10), and we previously reported that these gut-derived RELMs are apparently up-

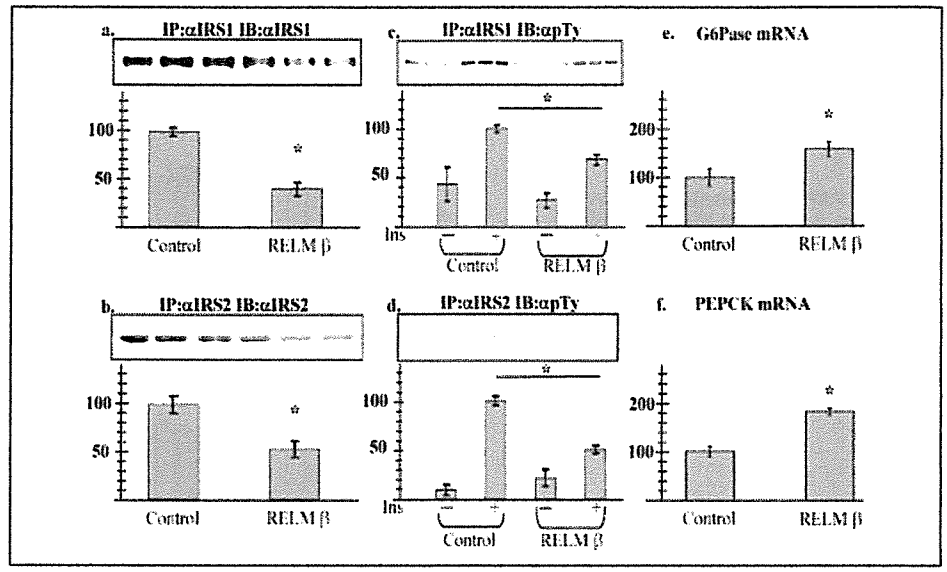

FIGURE 9. **IRS-1 and IRS-2 protein contents and phosphorylation by insulin in primary culture of hepatocytes, and mRNA levels of glucose-6-phosphatase and phosphoenolpyruvate carboxylase kinase.** Values are presented as means ± S.E. (*a*) and (*b*) compare the IRS protein contents. In *c* and *d*, phosphorylation of IRS; −, without insulin stimulation; +, with insulin stimulation. mRNA amount of glucose-6-phosphatase (*e*) and mRNA amount of phosphoenolpyruvate carboxylase kinase (*f*) are corrected by actin mRNA amount as the internal control; *scale* represents the percentage of control (without RELMβ). *, $p < 0.05$ for the condition without RELMβ (*Control*) *versus* with RELMβ (*RELMβ*). Each experiment was performed at least three times.

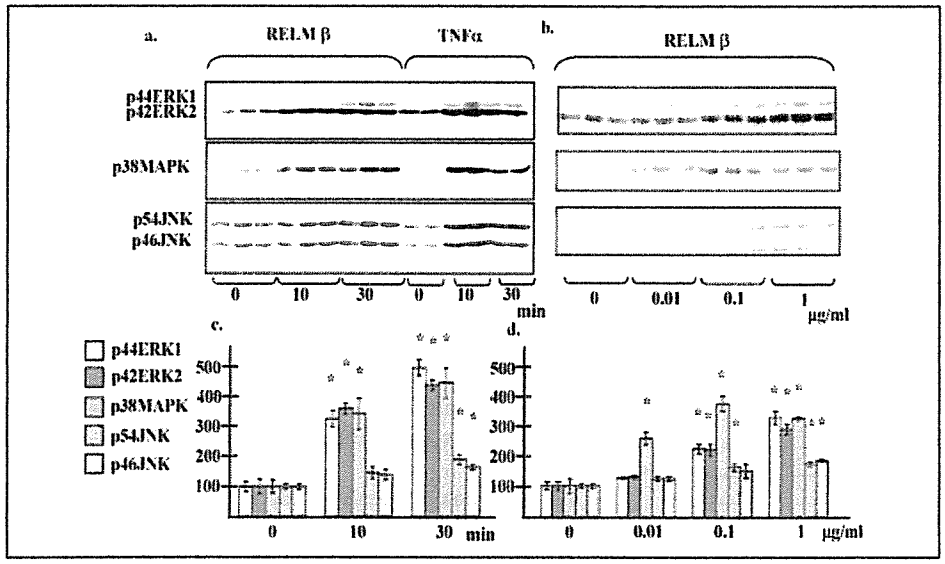

FIGURE 10. **MAPK phosphorylations in response to RELMβ stimulation in primary hepatocytes.** Western blots for phosho-p44/p42(ERK1/2), phospho-p38, and phospho-p54/p46(SAPK/JNK) were performed with: *a*, 10 or 30 min of RELMβ and tumor necrosis factor α stimulation; *b*, 0.01, 0.1, or 1 μl/ml RELMβ stimulation; *c*, densitometry of *a*; *d*, densitometry of *b*. Values are presented as means ± S.E. Each condition was examined 3–6 times. The *scale* represents the percentage of control. Statistical significance is indicated by an *asterisk*: *, $p < 0.05$ for the condition without RELMβ (*Control*) *versus* with RELMβ (*RELMβ*).

regulated in insulin-resistant rodent models. Thus, we speculated that the gastrointestinal tract might regulate insulin sensitivity by secreting these RELMs into the circulation in response to intestinal circumstances, *i.e.* inflammation, the food intake amount, and/or the nutritional contents of the food. Based on this hypothesis, this study was designed to answer questions as to whether or not the increased expression of gut-derived RELMβ actually induces insulin resistance, and if so, what molecular mechanisms underlie this regulation. To answer these questions, we generated transgenic mice with hepatic RELMβ overexpression, because overexpression in the liver is a commonly used method of investigating the chronic functions of several hormones, including leptin, growth hormone, and so on.

We speculate that RELMβ might possess dual roles; one in the circulation and the other in the gut. RELMβ functioning in the gut would be excreted into the stool. We consider hepatic RELMβ-overexpressing mice to be useful for investigating the role of RELMβ in the circulation, because overexpressing RELMβ in the liver, assuming a high focal concentration, would mimic the physiological pattern of RELMβ concentrations, because RELMβ probably initially flows into the liver via the portal vein.

We first demonstrated both line 1 and line 2 RELMβ transgenic mice, on a high fat diet, to phenotypically show hyperglycemia, hyperlipidemia, and hyperinsulinemia. Taking the data for line 2 into consideration, it seems that a relatively small increase in RELMβ expression can induce significant insulin resistance, which suggests that the increased serum RELMβ concentrations observed in the insulin resistant rodent models are physiologically significant. The consequent islet hyperplasia was considered to be due to prolonged insulin resistance. However, on the other hand, it should be noted that, when the mice were fed a normal diet, these metabolic abnormalities did not become overt even in the highly RELMβ-overexpressing line (line 1). This finding suggests that RELMβ itself induces a limited degree of insulin resistance that is not sufficient to cause overt diabetes or hyperlipidemia. Some additional factor(s) causing insulin resistance (in the case of our experiments, the high fat diet feeding) in addition to the increased serum RELMβ concentration would be necessary to induce diabetes or hyperlipidemia. It is also reasonable to regard increased RELMβ expression as just one of several independent molecular mechanisms underlying high fat diet insulin resistance.

Next, we demonstrated the presence of hepatic insulin resistance in

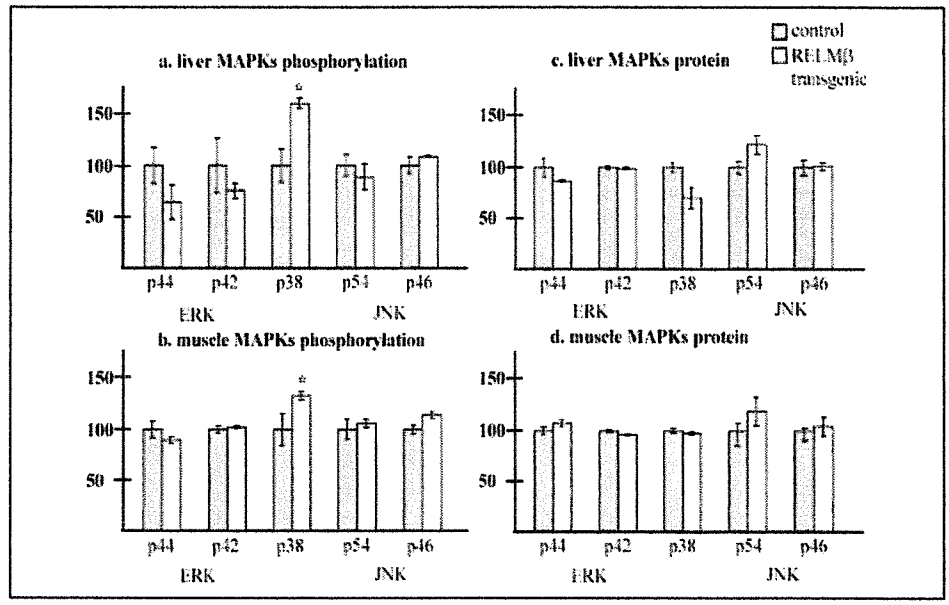

FIGURE 11. **MAPK phosphorylations and protein levels from 3-month-old RELMβ-overexpressing line 1 mice that had been fed a high fat diet, after an overnight fast.** Western blots for phosho-p44/p42(ERK1/2), p44/42, phospho-p38, p38, phospho-p54/p46(SAPK/JNK), and p54/p46 were performed. Each condition was examined in triplicate. The *scale* represents the percentage of control. Statistical significance is indicated by an *asterisk*: *, $p < 0.05$ for control mice *versus* transgenic mice.

TABLE THREE

mRNA levels of key lipid metabolic enzymes in the liver, measured using ribonuclease protection assay (RPA) using RELMβ overexpressing line 1 mice, at the age of 3 months, which had been fed a high fat diet for 4 weeks

Values are corrected by actin mRNA levels and by mean values of control mice as the standard (1.00 as standard mean value).

	Control	RELMβ trangenic
LDLR	1.00 ± 0.09	1.02 ± 0.06
PPARα	1.00 ± 0.13	0.72 ± 0.03
CPT1	1.00 ± 0.07	0.77 ± 0.07[a]
SREBP-1a	1.00 ± 0.08	0.98 ± 0.08
SREBP-1c	1.00 ± 0.17	0.92 ± 0.08
ACC	1.00 ± 0.04	1.09 ± 0.01[a]
FAS	1.00 ± 0.09	1.60 ± 0.34[a]
SCD1	1.00 ± 0.20	1.03 ± 0.15

[a] $p < 0.05$.

RELMβ transgenic mice, maintained on a high fat diet, by hyperinsulinemic glucose clamp test, which showed markedly increased hepatic glucose output while glucose utilization was intact. The pyruvate tolerance test, which reflects hepatic gluconeogenesis, yielded complementary results, because pyruvate is a substrate for gluconeogenesis (17). In contrast, we did not find changes in insulin-induced glucose transport activity in either peripheral tissues *in vivo*, or in isolated skeletal muscles *in vitro* from RELMβ transgenic as compared with control mice. Indeed, histochemical analysis revealed fatty livers in the RELMβ transgenic mice, although there was no obvious obesity at the time of sacrifice. Thus, it seems that glucose intolerance and hyperlipidemia in RELMβ transgenic mice are attributable mainly to hepatic insulin resistance. There is a curious discrepancy between the apparent insulin resistance in the insulin signaling pathway (*e.g.* insulin-induced PI 3-kinase activity) and unchanged insulin-induced glucose uptake by muscle, suggesting one or more compensatory mechanisms involving insulin-induced glucose transport, although this remains entirely speculative. In view of organ cross-talk, primary hepatic insulin resistance might affect glucose uptake in other peripheral tissues.

Subsequently, to elucidate whether or not the contribution of RELMβ to hepatic insulin resistance is direct, and what changes in signal transduction are induced by RELMβ, we performed experiments using primary cultured hepatocytes. Importantly, the expressions of IRS-1 and IRS-2 were demonstrated to be down-regulated in RELMβ-treated hepatocytes as well as liver and muscle tissues from RELMβ transgenic mice. In good agreement with the decreased IRS-1 and IRS-2 contents, PI 3-kinase activities associated with IRS-1 and IRS-2 and Akt activation, which are reportedly essential for insulin-induced metabolic actions, were also attenuated. These findings suggest that RELMβ functions directly in insulin-sensitive cells such as hepatocytes to suppress insulin signaling rather than as a consequence of hepatic lipid accumulation or of altered functions of other tissues such as adipose. The pattern of change in IRS protein contents is similar to that of *ob/ob* mice (32). Given the elevated serum concentration of RELMβ in the *ob/ob* mice, it may be reasonable to consider the elevated serum RELMβ concentration to at least contribute to the decreased IRS-1 and IRS-2 contents.

The next question concerns which type of signal transduction induced by RELMβ is involved in suppressing insulin signaling. Several previous studies have confirmed that the activation of ERK-1/2 or p38 MAPK leads to down-regulation of IRS-1 and IRS-2 (26). The activated JNK reportedly phosphorylates the serine residue in IRS-1 and suppresses insulin-induced PI 3-kinase activation. Thus, we investigated the effect of RELMβ on MAPK signaling using primary cultured hepatocytes. We found that ERK1/2, p38, and SAPK/JNK are phosphorylated in response to RELMβ. It was also recently reported that resistin phosphorylates and activates ERK-1/2 and p38 in smooth muscle cells (33). Thus, resistin and RELMβ are likely to have the same function. In addition, a significant increase in p38, but not ERK or JNK, phosphorylation was observed in both liver and muscle tissues of RELMβ transgenic mice. Because stimulation with RELMβ is constitutive in transgenic mice, we speculated that the effect of RELMβ might be difficult to detect but our results were consistent with those obtained using primary cultured hepatocytes.

Lipid metabolism remains an important issue. Some hepatic lipolytic and lipogenic enzymes were altered to promote lipid accumulation in the liver. These modest changes apparently reflect the moderate hyperlipidemia and liver steatosis of RELMβ transgenic mice. However, it is noteworthy that the key transcriptional factor, SREBP-1c, regulating lipid synthesis was not altered. The activation of p38 and other MAPKs

by RELMβ may be involved in regulating lipid metabolism as previously reported (34–36).

Our results suggest that chronic stimulation by RELMβ causes glucose intolerance and hyperlipidemia associated with impaired insulin signaling, and the activations of three MAPKs are probably involved in this insulin signaling suppression. Although our findings suggest the importance of increased RELMβ expression in the pathogenesis of diabetes and hyperlipidemia, there are still limitations in interpreting the physiological role of RELMβ in the pathogenesis of insulin resistance, because glucose homeostasis is modestly impaired in RELMβ transgenic mice relative to control mice, on a high fat diet only. Thus, further studies are necessary to elucidate how much RELMβ actually contributes to insulin resistance caused by various factors. For example, the percentages of RELMβ present in circulating blood as monomers, dimers, and hexamers and the biological activities of each form, should be determined. Identification of the specific RELMβ receptor as well as the relationship between serum RELMβ and insulin sensitivity in humans are important. Further studies may reveal that RELMβ is a potentially useful marker for assessing insulin resistance associated with obesity and may serve as a target for novel anti-diabetic agents.

REFERENCES

1. Steppan, C. M., Bailey, S. T., Bhat, S., Brown, E. J., Banerjee, R. R., Wright, C. M., Patel, H. R., Ahima, R. S., and Lazar, M. A. (2001) *Nature* **409,** 307–312
2. Kim, K. H., Lee, K., Moon, Y. S., and Sul, H. S. (2001) *J. Biol. Chem.* **276,** 11252–11256
3. Moon, B., Kwan, J. J., Duddy, N., Sweeney, G., and Begum, N. (2003) *Am. J. Phys-iol.* **285,** E106–E115
4. Banerjee, R. R., Rangwala, S. M., Shapiro, J. S., Rich, A. S., Rhoades, B., Qi, Y., Wang, J., Rajala, M. W., Pocai, A., Scherer, P. E., Steppan, C. M., Ahima, R. S., Obici, S., Rossetti, L., and Lazar, M. A. (2004) *Science.* **303,** 1195–1198
5. Rangwala, S. M., Rich, A. S., Rhoades, B., Shapiro, J. S., Obici, S., Rossetti, L., and Lazar, M. A. (2004) *Diabetes* **53,** 1937–1941
6. Satoh, H., Nguyen, M. T., Miles, P. D., Imamura, T., Usui, I., and Olefsky, J. M. (2004) *J. Clin. Invest.* **114,** 224–231
7. Fehmann, H. C., and Heyn, J. (2002) *Horm. Metab. Res.* **34,** 671–673
8. Lee, J. H., Chan, J. L., Yiannakouris, N., Kontogianni, M., Estrada, E., Seip, R., Orlova, C., and Mantzoros, C. S. (2003) *J. Clin. Endocrinol. Metab.* **88,** 4848–4856
9. Steppan, C. M., Brown, E. J., Wright, C. M., Bhat, S., Banerjee, R. R., Dai, C. Y., Enders, G. H., Silberg, D. G., Wen, X., Wu, G. D., and Lazar, M. A. (2001) *Proc. Natl. Acad. Sci. U. S. A.* **98,** 502–506
10. Chumakov, A. M., Kubota, T., Walter, S., and Koeffler, H. P. (2004) *Oncogene* **23,** 3414–3425
11. Rajala, M. W., Obici, S., Scherer, P. E., and Rossetti, L. (2003) *J. Clin. Invest.* **111,** 225–230
12. Shojima, N., Ogihara, T., Inukai, K., Fujishiro, M., Sakoda, H., Kushiyama, A., Katagiri, H., Anai, M., Ono, H., Fukushima, Y., Horike, N., Viana, A. Y., Uchijima, Y., Kurihara, H., and Asano, T. (2005) *Diabetologia* **48,** 984–992
13. Ono, H., Shimano, H., Katagiri, H., Yahagi, N., Sakoda, H., Onishi, Y., Anai, M., Ogihara, T., Fujishiro, M., Viana, A. Y., Fukushima, Y., Abe, M., Shojima, N., Kikuchi, M., Yamada, N., Oka, Y., and Asano, T. (2003) *Diabetes* **52,** 2905–2913
14. Anai, M., Funaki, M., Ogihara, T., Kanda, A., Onishi, Y., Sakoda, H., Inukai, K., Nawano, M., Fukushima, Y., Yazaki, Y., Kikuchi, M., Oka, Y., and Asano, T. (1999) *Diabetes* **48,** 158–169
15. Folch, J., Lees, M., and Sloane Stanley, G. H. (1957) *J. Biol. Chem.* **226,** 497–509
16. Bergmeyer, H., Bergmeyer, J., and Grassl, M. (1984) *Methods of Enzymatic Analys-is, 3rd ed.*, Wiley, Hoboken, NJ, pp. 11–18
17. Miyake, K., Ogawa, W., Matsumoto, M., Nakamura, T., Sakaue, H., and Kasuga, M. (2002) *J. Clin. Invest.* **110,** 1483–1491
18. Onishi, Y., Honda, M., Ogihara, T., Sakoda, H., Anai, M., Fujishiro, M., Ono, H., Shojima, N., Fukushima, Y., Inukai, K., Katagiri, H., Kikuchi, M., Oka, Y., and Asano, T. (2003) *Biochem. Biophys-. Res. Commun.* **303,** 788–794
19. Miles, P. D., Barak, Y., Evans, R. M., and Olefsky, J. M. (2003) *Am. J. Phys-iol.* **284,** E618–E626
20. Fueger, P. T., Bracy, D. P., Malabanan, C. M., Pencek, R. R., Granner, D. K., and Wasserman, D. H. (2004) *Diabetes* **53** 306–314
21. Fisher, S. J., and Kahn, C. R. (2003) *J. Clin. Invest.* **111,** 463–468
22. Ogihara, T., Shin, B. C., Anai, M., Katagiri, H., Inukai, K., Funaki, M., Fukushima, Y., Ishihara, H., Takata, K., Kikuchi, M., Yazaki, Y., Oka, Y., and Asano, T. (1997) *J. Biol. Chem.* **272,** 12868–12873
23. Ogihara, T., Asano, T., Katagiri, H., Sakoda, H., Anai, M., Shojima, N., Ono, H., Fujishiro, M., Kushiyama, A., Fukushima, Y., Kikuchi, M., Noguchi, N., Aburatani, H., Gotoh, Y., Komuro, I., and Fujita, T. (2004) *Diabetologia* **47,** 794–805
24. Sakoda, H., Ogihara, T., Anai, M., Fujishiro, M., Ono, H., Onishi, Y., Katagiri, H., Abe, M., Fukushima, Y., Shojima, N., Inukai, K., Kikuchi, M., Oka, Y., and Asano, T. (2002) *Am. J. Phys-iol.* **282,** E1239–E1244
25. Sakoda, H., Gotoh, Y., Katagiri, H., Kurokawa, M., Ono, H., Onishi, Y., Anai, M., Ogihara, T., Fujishiro, M., Fukushima, Y., Abe, M., Shojima, N., Kikuchi, M., Oka, Y., Hirai, H., and Asano, T. (2003) *J. Biol. Chem.* **278,** 25802–25807
26. Fujishiro, M., Gotoh, Y., Katagiri, H., Sakoda, H., Ogihara, T., Anai, M., Onishi, Y., Ono, H., Abe, M., Shojima, N., Fukushima, Y., Kikuchi, M., Oka, Y., and Asano, T. (2003) *Mol. Endocrinol.* **17,** 487–497
27. Tomimoto, S., Hashimoto, H., Shintani, N., Yamamoto, K., Kawabata, Y., Hamagami, K., Yamagata, K., Miyagawa, J., and Baba, A. (2004) *J. Pharmacol. Exp. Ther.* **309,** 796–803
28. Kojima, M., Hosoda, H., Date, Y., Nakazato, M., Matsuo, H., and Kangawa, K. (1999) *Nature.* **402,** 656–660
29. Miyawaki, K., Yamada, Y., Yano, H., Niwa, H., Ban, N., Ihara, Y., Kubota, A., Fujimoto, S., Kajikawa, M., Kuroe, A., Tsuda, K., Hashimoto, H., Yamashita, T., Jomori, T., Tashiro, F., Miyazaki, J., and Seino, Y. (1999) *Proc. Natl. Acad. Sci. U. S. A.* **96,** 14843–14847
30. Murata, M., Okimura, Y., Iida, K., Matsumoto, M., Sowa, H., Kaji, H., Kojima, M., Kangawa, K., and Chihara, K. (2002) *J. Biol. Chem.* **277,** 5667–5674
31. Mooney, M. H., Abdel-Wahab, Y. H., McKillop, A. M., O'Harte, F. P., and Flatt, P. R. (2002) *Biochim. Biophys-. Acta* **1569,** 75–80
32. Kerouz, N. J., Horsch, D., Pons, S., and Kahn, C. R. (1997) *J. Clin. Invest.* **100,** 3164–3172
33. Calabro, P., Samudio, I., Willerson, J. T., and Yeh, E. T. (2004) *Circulation* **110,** 3335–3340
34. Samuel, V. T., Liu, Z. X., Qu, X., Elder, B. D., Bilz, S., Befroy, D., Romanelli, A. J., and Shulman, G. I. (2004) *J. Biol. Chem.* **279,** 32345–32353
35. Mehta, K. D., and Miller, L. (1999) *Trends Cardiovasc. Med.* **9,** 201–205
36. Kapoor, G. S., Atkins, B. A., and Mehta, K. D. (2002) *Mol. Cell Biochem.* **236,** 13–22

THE JOURNAL OF BIOLOGICAL CHEMISTRY VOL. 280, NO. 47, pp. 39609–39615, November 25, 2005
© 2005 by The American Society for Biochemistry and Molecular Biology, Inc. Printed in the U.S.A.

WFS1 Is a Novel Component of the Unfolded Protein Response and Maintains Homeostasis of the Endoplasmic Reticulum in Pancreatic β-Cells*

Received for publication, July 8, 2005, and in revised form, September 27, 2005 Published, JBC Papers in Press, September 29, 2005, DOI 10.1074/jbc.M507426200

Sonya G. Fonseca[‡], Mariko Fukuma[‡1], Kathryn L. Lipson[‡], Linh X. Nguyen[‡], Jenny R. Allen[‡], Yoshitomo Oka[§], and Fumihiko Urano[‡¶2]

From the [‡]Program in Gene Function and Expression and [¶]Program in Molecular Medicine, University of Massachusetts Medical School, Worcester, Massachusetts 01605 and [§]Division of Molecular Metabolism and Diabetes, Tohoku University Graduate School of Medicine, Sendai 980-8575, Japan

In Wolfram syndrome, a rare form of juvenile diabetes, pancreatic β-cell death is not accompanied by an autoimmune response. Although it has been reported that mutations in the *WFS1* gene are responsible for the development of this syndrome, the precise molecular mechanisms underlying β-cell death caused by the *WFS1* mutations remain unknown. Here we report that WFS1 is a novel component of the unfolded protein response and has an important function in maintaining homeostasis of the endoplasmic reticulum (ER) in pancreatic β-cells. WFS1 encodes a transmembrane glycoprotein in the ER. WFS1 mRNA and protein are induced by ER stress. The expression of WFS1 is regulated by inositol requiring 1 and PKR-like ER kinase, central regulators of the unfolded protein response. WFS1 is normally up-regulated during insulin secretion, whereas inactivation of WFS1 in β-cells causes ER stress and β-cell dysfunction. These results indicate that the pathogenesis of Wolfram syndrome involves chronic ER stress in pancreatic β-cells caused by the loss of function of WFS1.

In 1938, Wolfram and Wagener (1) analyzed four siblings with the combination of juvenile diabetes and optic atrophy, thus providing the first report of Wolfram syndrome. Because a significant portion of patients with Wolfram syndrome develop diabetes insipidus and auditory nerve deafness, this syndrome is also referred to as the diabetes insipidus, diabetes mellitus, optic atrophy, and deafness syndrome (2, 3). Its pathogenesis is still unknown.

Although patients with Wolfram syndrome are not generally obese and do not have insulitis, the β-cells in their pancreatic islets are selectively destroyed (4). Families that exhibit Wolfram syndrome share mutations in a gene encoding the WFS1 protein, a transmembrane protein in the endoplasmic reticulum (ER)[3] (5, 6). WFS1 serves as an ER calcium channel (7), suggesting that this molecule may have a function in ER homeostasis. Therefore, inactivation of WFS1 may cause imbalances in ER homeostasis.

The ER is an important cellular compartment for the folding of newly synthesized secretory proteins such as proinsulin. Imbalance in ER homeostasis elicits stress in this organelle. ER stress is defined as an imbalance between the actual folding capacity of the ER and the demand placed on this organelle. The unfolded protein response (UPR), an adaptive response that counteracts ER stress, has three components as follows: gene expression, translational attenuation, and ER-associated protein degradation system (8–10). Accumulating evidence suggests that a high level of ER stress or defective ER stress signaling (*i.e.* the UPR) causes β-cell death during the development of diabetes (9, 11–13).

Inositol requiring 1 (IRE1), a sensor for unfolded and misfolded proteins in the ER, is a central regulator of the UPR. IRE1α, which is expressed ubiquitously, has a high level of expression in the pancreas and placenta (14, 15); IRE1β is expressed only in epithelial cells of the gastrointestinal tract (16, 17). The presence of unfolded proteins in the ER causes dimerization, trans-autophosphorylation, and consequent activation of IRE1. Activated IRE1 splices XBP-1 (X-box binding protein-1) mRNA, leading to synthesis of the active transcription factor XBP-1 and up-regulation of UPR genes (18, 19). In contrast, prolonged ER stress activates the cell-death pathway through IRE1. Under chronic ER stress, IRE1 recruits tumor necrosis factor receptor-associated factor 2 (20), which activates apoptosis-signaling kinase 1 (ASK1) (21, 22). Activated ASK1 leads to the activation of c-Jun N-terminal protein kinase and, in the presence of extreme ER stress, induces apoptosis (23). It has been suggested that this pathway is important for insulin resistance in patients with type 2 diabetes (24). Obesity causes ER stress in the liver and leads to hyperactivation of c-Jun N-terminal protein kinase signaling. This causes serine phosphorylation of insulin receptor substrate-1 and inhibits insulin action in liver cells. In addition, tumor necrosis factor receptor-associated factor 2 recruitment by IRE1 causes clustering and activation of caspase-12 at the ER membrane (25). Activated caspase-12 induces apoptosis under pathological ER stress conditions (26).

Two more upstream components in the UPR, PKR-like ER kinase (PERK) and activating transcription factor 6 (ATF6) (27–29), are also sensors of unfolded or misfolded proteins and are activated by the accumulation of such proteins in the ER. PERK is highly expressed in pancreatic islets (29, 30). Activated PERK phosphorylates the α subunit of eukaryotic translation initiation factor 2 (eIF2α), which leads to the attenuation of general protein translation. This reduces the ER workload and protects cells from apoptosis resulting from ER stress (31). In Wolcott-Rallison syndrome, a rare form of juvenile diabetes, mutations

* This work was supported by NIDDK Grant 1R01DK067493-01 from the National Institutes of Health, the National Institutes of Health Diabetes and Endocrinology Research Center at the University of Massachusetts Medical School, a Worcester Foundation award, a Juvenile Diabetes Research Foundation Innovative grant, an American Diabetes Association Innovation grant, and an Iacocca Foundation grant (to F. U.). The costs of publication of this article were defrayed in part by the payment of page charges. This article must therefore be hereby marked "*advertisement*" in accordance with 18 U.S.C. Section 1734 solely to indicate this fact.

[1] Present address: Dept. of Pathology, Keio University School of Medicine, Tokyo 160-8582, Japan.

[2] To whom correspondence should be addressed: Program in Gene Function and Expression, University of Massachusetts Medical School, Worcester, MA 01605-2324. Tel.: 508-856-6012; Fax: 508-856-4650; E-mail: Fumihiko.Urano@umassmed.edu.

[3] The abbreviations used are: ER, endoplasmic reticulum; UPR, unfolded protein response; IRE1, inositol requiring 1; PERK, PKR-like ER kinase; EIF2α, eukaryotic translation initiation factor 2; siRNA, small interfering RNA; ATF6, activating transcription factor 6.